

# **Iodine distribution, speciation and mobility in volcanic soils of a tropical forest – a case study from Costa Rica**

---

Master thesis at the Technical University of Braunschweig  
Faculty of Architecture, Civil Engineering and Environmental Sciences

Institute of Geoecology

Professorship for Environmental Geochemistry  
& Professorship for Soil Science and Soil Physics

Katrin Schulz

Matriculation no.: 4663845

Braunschweig,

March 29<sup>th</sup>, 2018

Supervisor: Prof. Dr. Harald Biester

Co-Supervisor: Apl. Prof. Dr. Rolf Nieder



## Declaration

I declare that I have authored this thesis independently, that I have not used other than the declared sources, and that I have explicitly marked all material which has been quoted either literally or by content from the used sources.

## Eigenständigkeitserklärung

Hiermit versichere ich, die vorliegende Masterarbeit eigenständig und nur unter Verwendung der im Literaturverzeichnis aufgeführten Quellen angefertigt zu haben. Jegliches Material, das direkt oder indirekt zitiert wurde, habe ich explizit gekennzeichnet.

Declared by: Katrin Schulz, born on 12.03.1992 in Stuttgart, Germany

Braunschweig, .....

Signature: .....

# Table of Contents

List of Tables .....	III
List of Figures .....	IV
List of Appendix Figures and Tables.....	V
List of Abbreviations .....	VI
Assignment .....	1
Abstract.....	2
Zusammenfassung .....	3
Acknowledgements.....	4
1 Introduction .....	5
1.1 Significance of iodine .....	5
1.2 Iodine cycling and -chemistry in soils .....	5
1.2.1 The path of I from oceans to soils.....	5
1.2.2 I sorption in soils .....	7
1.2.3 I mobility and volatilisation from soils.....	8
1.3 Tropical systems and volcanic soils.....	9
1.3.1 Characteristics of tropical forest ecosystems.....	9
1.3.2 Tropical volcanic soils – Characteristics and pedogenesis.....	9
1.4 Aims and hypotheses .....	10
2 Methods and study site.....	11
2.1 Study site .....	11
2.2 Sampling sites, field parameters and sampling technique .....	12
2.2.1 Solid soil samples .....	12
2.2.2 Soil pore water sampling .....	13
2.3 pH value, water content and texture .....	13
2.4 Soil characterisation.....	14
2.5 Chemical analysis .....	19
2.6 Batch leaching experiments.....	20
2.7 Statistical analysis.....	20

3	Results .....	21
3.1	Solid soil samples .....	21
3.1.1	I and Br concentrations in solid samples .....	21
3.1.2	C and Fe concentrations in solid samples .....	22
3.1.3	Quality of solid soil sample analyses .....	24
3.2	Leachates.....	25
3.2.1	I and Br concentrations in leachates .....	25
3.2.2	DOC and Fe concentrations in leachates .....	27
3.2.3	Quality of leachates and pore water analyses .....	27
3.3	Correlations.....	28
3.3.1	Correlations of I and Br with C and DOC .....	28
3.3.2	Correlations of I, Br and C with other elements .....	28
3.4	I/Br ratios .....	30
3.5	Spatial differences in I, Br, C and Fe concentrations.....	31
3.6	Accumulation vs. depletion of nutrients .....	33
3.7	Pore water samples – Depth profiles of element concentrations .....	34
4	Discussion .....	36
4.1	I and Br status in the soils of the ReBAMB.....	36
4.1.1	High I and Br contents in solid soil samples and low leachability .....	36
4.1.2	I and Br accumulation in soils.....	36
4.2	Processes determining I and Br accumulation in the soils of the ReBAMB .....	37
4.2.1	I and Br sources to soils.....	37
4.2.2	Sorption of I and Br to OM.....	38
4.2.3	Association of other elements with OM .....	39
4.2.4	Mobilisation of I and Br through DOC .....	39
4.2.5	Mobilisation of other elements through DOC.....	40
4.2.6	Low DOC concentrations due to DOC stabilisation and decomposition.....	40
4.2.7	Stabilisation of dissolved organic I- and Br complexes by Fe-Oxides .....	41
4.2.8	The role of soil texture, bulk density and air temperature for I and Br fixation ..	42
4.2.9	I and Br volatilisation and plant uptake .....	43

4.2.10	Role of soil erosion for I and Br distribution.....	43
4.2.11	I- and Br accumulation vs. nutrient depletion.....	44
4.2.12	Comparison of pore water samples and leachates .....	44
4.3	Comparison of <i>I</i> and Br soil chemistry .....	45
4.3.1	Differences in I and Br soil chemistry – Correlations and I/Br ratios .....	45
4.3.2	I and Br species.....	46
5	Outlook.....	47
6	Conclusion .....	47
	References.....	49
	Appendix.....	56
	Soil profiles .....	56
	Nutrient concentrations .....	59



## List of Tables

Table 1: General soil properties of all soil profiles on slopes L and R, assessed according to the German soil classification KA5 (Eckelmann et al., 2006).....	14
Table 2: Soil characteristics of profiles on slope L, assessed according to German classification KA5 (Eckelmann et al., 2006) and WRB soil types. ....	17
Table 3: Soil characteristics of profiles on slope R, assessed according to German classification KA5 (Eckelmann et al., 2006) and WRB soil types. ....	18
Table 4: pH values in water ( $\text{pH}_{\text{H}_2\text{O}}$ ) and 0.01 M calcium chloride solution ( $\text{pH}_{\text{CaCl}_2}$ ) and gravimetric water content of profiles L2, R2 and R4.....	19
Table 5: Reference materials for solid soil analyses with certified values (CV) and measured values (MV). ....	24
Table 6: Reference materials for liquid sample analyses with certified values (CV) and measured values (MV) for leachates (MV 1) and pore water samples (MV 2).....	27
Table 7: Spearman correlation coefficients of <i>I</i> , Br and C and all measured elements in solid samples, non-significant correlations are written in grey. ....	29
Table 8: Spearman correlation coefficients of <i>I</i> , Br and DOC and all measured elements in leachates, non-significant correlations are written in grey. ....	29
Table 9: Typical values and mean of main- and trace nutrient concentrations in solid soil samples, high mean concentrations in relation to typical values are printed in italic, low mean concentrations in bold. ....	34
Table 10: Typical values, mean and median Iron (Fe) [ $\mu\text{g L}^{-1}$ ], Chloride ( $\text{Cl}^-$ ) [ $\text{mg L}^{-1}$ ], Nitrate ( $\text{NO}_3^-$ ) [ $\text{mg L}^{-1}$ ] and Sulfate ( $\text{SO}_4^{2-}$ ) [ $\text{mg L}^{-1}$ ] concentrations in leachates. Low mean concentrations in relation to typical values are marked in bold.....	34
Table 11: Dissolved organic carbon (DOC), Iodine ( <i>I</i> ), Bromine (Br), Iron (Fe), Chloride ( $\text{Cl}^-$ ), Nitrate ( $\text{NO}_3^-$ ) and Sulfate ( $\text{SO}_4^{2-}$ ) in pore water samples. ....	35

## List of Figures

Figure 1: Overview of iodine cycling in the environment. ....	6
Figure 2: Iodine covalently bound to aromatic structure of fulvic acid (adapted from Moulin et al., 2001).....	8
Figure 3: Location, digital elevation model of the study area, ReBAMB, Costa Rica. ....	11
Figure 4: Left: Overview of the San Lorencito catchment, ReBAMB, Costa Rica; Right: location of soil profiles on slope L and R, Research Station (house) and Weather Station (triangle).....	12
Figure 5: Summary of sample preparation and analytical methods for solid soil samples, soil pore water and leachates. ....	13
Figure 6: Soil profile L3, Colluvic Cambisol, ReBAMB, Costa Rica, June 2017.....	15
Figure 7: Soil profile R2, Haplic Cambisol, ReBAMB, Costa Rica, June 2017. ....	16
Figure 8: Iodine ( <i>I</i> ) and bromine ( <i>Br</i> ) concentrations in solid soil samples [ $\text{mg kg}^{-1}$ ] of profiles L1-L4 and R1-R5, shown at the average depth for each sampled horizon (Table 2 and Table 3). ....	22
Figure 9: Carbon ( <i>C</i> ) concentrations in solid soil samples [ $\text{mg kg}^{-1}$ ] and leachates [ $\text{mg L}^{-1}$ ] in profiles L1-L4 and R1-R5, shown at the average depth for each sampled horizon (Table 2 and Table 3). ....	23
Figure 10: Iron ( <i>Fe</i> ) concentrations in solid soil samples [ $\text{g kg}^{-1}$ ] and leachates [ $\mu\text{g L}^{-1}$ ] in profiles L1-L4 and R1-R5, shown at the average depth for each sampled horizon (Table 2 and Table 3). ....	23
Figure 11: Iodine ( <i>I</i> ) and Bromine ( <i>Br</i> ) concentrations in leachates [ $\mu\text{g L}^{-1}$ ] of profiles L1-L4 and R1-R5, shown at the average depth for each sampled horizon (Table 2 and Table 3), with x-axis scale set to 50 for L2. ....	26
Figure 12: Percentage of leachable fraction of <i>I</i> and <i>Br</i> , calculated for dry soil samples of profiles L1-4 and R1-5, shown at the average depth for each sampled horizon (Table 2 and Table 3), with x-axis scale set to 0.6 % for L2.....	26
Figure 13: Spearman correlation of <i>I</i> - <i>C</i> , <i>I</i> -DOC, <i>Br</i> - <i>C</i> and <i>Br</i> -DOC and Spearman correlation coefficient ( $\rho$ ), with * $p < 0.05$ , ** $p < 0.01$ and *** $p < 0.001$ .....	28
Figure 14: Iodine-bromine-ratios in rain water sample (0.3), solid soil samples and leachates in profiles L1-L4 and R1-R5, shown at the average depth for each sampled horizon (Table 2 and Table 3). ....	31
Figure 15: Boxplot of iodine ( <i>I</i> ) [ $\text{mg kg}^{-1}$ ], bromine ( <i>Br</i> ) [ $\text{mg kg}^{-1}$ ], carbon ( <i>C</i> ) [ $\text{g kg}^{-1}$ ] and iron ( <i>Fe</i> ) [ $\text{g kg}^{-1}$ ] concentrations in solid samples of topsoil horizons (5-6 cm) on slope L and R, shown at the average depth for each sampled horizon (Table 2 and Table 3), black lines show medians, black dots represent data points, boxes cover the 25 % and 75 % quartile, whiskers extend to 1.5-fold extension of the respective box. ....	32

Figure 16: Boxplot of iodine ( <i>I</i> ) [ $\mu\text{g L}^{-1}$ ], bromine (Br) [ $\mu\text{g L}^{-1}$ ], dissolved organic carbon (DOC) [ $\text{mg L}^{-1}$ ] and iron (Fe) [ $\mu\text{g L}^{-1}$ ] concentrations in solid samples of topsoil horizons (5-6 cm) on slope L and R, shown at the average depth for each sampled horizon (Table 2 and Table 3), black lines show medians, black dots represent data points, boxes cover the 25 % and 75 % quartile, whiskers extend to 1.5-fold extension of the respective box. ....	33
Figure 17: Overview of <i>I</i> chemistry in soils of the ReBAMB.....	48

## List of Appendix Figures and Tables

Appendix 1: Soil profiles L1 (left, Colluvic Cambisol) and L2 (right, Haplic Cambisol), ReBAMB, Costa Rica, June 2017.....	56
Appendix 2: Soil profiles L3 (left, Colluvic Cambisol) and L4 (right, Colluvic Cambisol), ReBAMB, Costa Rica, June 2017.....	57
Appendix 3: Soil profiles R1 (left, Cambisol) and R2 (right, Haplic Cambisol), ReBAMB, Costa Rica, June 2017.....	57
Appendix 4: Soil profiles R3 (left, Cambisol) and R4 (right, Dystric Cambisol), ReBAMB, Costa Rica, June 2017.....	58
Appendix 5: Soil profile R5 (Cambisol), ReBAMB, Costa Rica, June 2017.....	58
Appendix 6: Iron (Fe), Chloride ( $\text{Cl}^-$ ), Nitrate ( $\text{NO}_3^-$ ) and Sulfate ( $\text{SO}_4^{2-}$ ) concentrations in leachates.....	59
Appendix 7: Main- and trace nutrient concentrations in solid soil samples.....	60

## List of Abbreviations

<i>Abbreviation</i>	<i>Meaning</i>
Ah	Humified topsoil horizon
AhBw	Transitional horizon between Ah and Bw horizon
Bw	Weathered subsoil horizon
C*	Bedrock horizon in soil
CNS	Carbon Nitrogen Sulphur Analyser
COI	Colloidal organically bound iodine
DOC	Dissolved organic carbon
DOM	Dissolved organic matter
HPLC	High performance liquid chromatography
IC	Ion chromatography
ICP-MS	Inductively coupled Plasma mass spectrometry
ICP-OES	Inductively coupled Plasma optical emission spectrometry
IDD	Iodine deficiency disorders
IFP	Iodine fixation potential
II AhBw	Weathered Ah horizon on different substrate
L1-4	Soil profiles on slope L
OM	Organic matter
R1-5	Soil profiles on slope R
ReBAMB	Reserva Biologica Arturo Manuel Brenes
SOI	Soluble organic iodine
SOM	Soil organic matter
XRF	X-ray fluorescence spectrometry
$\rho$	Spearman correlation coefficient

## Assignment

Iodine is a trace element and micronutrient in terrestrial ecosystems. It plays a major role in regulating the metabolism in human cells through its involvement in the synthesis of thyroid hormones. Insufficient uptake can lead to iodine deficiency disorders (IDD) causing serious health problems, such as goitre or cretinism (Andersson et al., 2007). Therefore, it is important to understand the processes that determine its behaviour in the environment. In soils, iodine can bind to organic matter and iron (Shetaya et al., 2012). This determines if it is retained in the soil or washed out by percolating water.

The aim of this master thesis, is the investigation of iodine chemistry in an acidic volcanic soil in a tropical catchment in Costa Rica. And to examine the role of dissolved organic carbon in iodine mobilisation or retention. This is examined in the Antonio Manuel Brenes biological reserve (ReBAMB).

The thesis contains a chemical and physical characterisation of the soil in the ReBAMB in Costa Rica. This includes the acquisition of soil parameters in the field and the chemical analysis of solid soil samples and soil solution in the laboratory. Batch leaching experiments will be used to determine leachable iodine fractions. For analyses and quantification ICP-MS, ICP-OES, IC, TOC-Analyser, HPLC, CNS, XRF and a coupling of thermal iodine extraction and ICP-MS will be used.

The following questions will be addressed: How much and which form of iodine and carbon is present in the investigated soils? How high is their mobility? Are there relationships between iodine and other elements? Which processes can explain the distribution, mobility and retention of iodine and carbon in the soil?

Signature Prof. Dr. Harald Biester: .....

## Abstract

Iodine (*I*) is an essential trace element for regulating cell metabolism in humans. Insufficient uptake can lead to severe health consequences, such as goitre or cretinism. The mobility of *I* in terrestrial environments is closely related to that of dissolved organic carbon (DOC). The retention and mobilisation of *I* in soils in tropical ecosystems are poorly understood. This master thesis aims to reveal factors that determine *I* soil chemistry in tropical soils, to assess the role of DOC and provide a comparison of *I* and bromine (Br) soil chemistry. Soil samples and pore water samples from nine soil profiles were taken in a pristine tropical pre-montane rainforest in Costa Rica. The study area is characterised by steep slopes and former volcanic influence, including ash deposits, basaltic and andesitic bedrock. The water-soluble fractions of these elements were assessed by batch leaching experiments and pore water samples. Solid soil samples and leachates were analysed for *I*, Br, total carbon (C), dissolved organic carbon (DOC), nitrogen (N), iron (Fe) concentrations and different main- and trace elements.

*I* concentrations in solid soil samples were high (median: 69 mg kg<sup>-1</sup>), but the maximum water-soluble fraction was 0.4 %, only (median 0.01 %). The median Br concentration in solid soil samples was 71 mg kg<sup>-1</sup>, facing a maximum water leachable fraction of 0.6 % (median 0.04 %). C showed a maximum leachable dissolved organic carbon (DOC) proportion of 0.1 %. Leaching of *I*, Br and DOC was highest, but still poor, in topsoils, and comparatively low in subsoils. Spearman correlations for *I* and Br with C were positive and significant, but higher for leachates (*I*-DOC: 0.70, Br-DOC: 0.74) than for solid samples (*I*-C: 0.42, Br-C: 0.57). *I*/Br ratios indicated a stronger fixation of *I* and a higher mobility of Br in the investigated soils.

The findings suggest a rapid fixation of *I* and Br with C in organic matter (OM) rich topsoil horizons after the incorporation through rainfall. Small fractions are associated with DOC and transported to deeper soil horizons. There, DOC-*I* and DOC-Br associations are fixated by Fe-Oxides. Fixation of organic *I* and Br complexes by Fe-Oxides plays an important role in these soils. In conclusion, tropical soils with high contents of OM and Fe-Oxides provide a high fixation- and accumulation potential for *I* and receive immense *I* inputs due to high annual rainfall.

## Zusammenfassung

Iod (*I*) ist ein essentielles Spurenelement für die Regulation des menschlichen Zellstoffwechsels. *I*-Mangel kann zu gravierenden Gesundheitsschäden führen. Das Wissen über das Verhalten von *I* in tropischen Böden ist gering. Diese Masterarbeit soll Faktoren offenlegen, die Retentions- und Mobilisierungsprozesse bestimmen, die Rolle von gelöstem organischem Kohlenstoff (DOC) untersuchen und einen Vergleich des bodenchemischen Verhaltens von *I* und Brom (Br) bieten. Boden- und Porenwasserproben wurden aus neun Bodenprofilen in einem ungestörten, tropischen, prämontanen Regenwald in Costa Rica entnommen. Steile Hänge und ehemaliger vulkanischer Einfluss prägen das Untersuchungsgebiet. Die wasserlösliche Fraktion dieser Elemente wurde durch Schüttelversuche und die Porenwasserproben ermittelt. Laboranalysen der Flüssigproben und der Feststoffproben beinhalteten die Bestimmung von *I*, Br, Kohlenstoff (C), DOC, Eisen (Fe) Konzentrationen und Gehalte anderer Haupt- und Spurenelemente.

Die Ergebnisse zeigten hohe Gehalte an *I* (Median 69 mg kg<sup>-1</sup>), die maximale wasserlösliche Fraktion betrug jedoch nur 0.4 % (Median 0.01 %). Der Median der Br Konzentrationen in den Feststoffproben lag bei 71 mg kg<sup>-1</sup>, die maximale wasserlösliche Fraktion betrug 0.6 % (Median 0.04 %). C zeigte ebenfalls nur einen maximal wasserlöslichen Anteil von DOC von 0.1 %. Die stärkste, jedoch immer noch geringe, Auswaschung von *I*, Br und DOC wurde im Oberboden beobachtet, während sie im Unterboden vergleichsweise gering war. Die Spearman Korrelationen für *I* und Br mit C waren positiv und signifikant, die Korrelationskoeffizienten lagen in den Eluaten (*I*-DOC: 0.70, Br-DOC: 0.74) höher als in den Feststoffproben (*I*-C: 0.42, Br-C: 0.57). Das *I*/Br Verhältnis zeigte eine stärkere Fixierung von *I* und eine stärkere Auswaschung von Br aus den untersuchten Böden.

Die Ergebnisse deuten auf eine schnelle Fixierung von *I* und Br durch die organische Substanz nach dem Eintrag über den Niederschlag hin. Geringe Anteile scheinen, hauptsächlich in Verbindung mit DOC, in tiefere Bodenhorizonte transportiert zu werden. Dort werden die DOC-*I* und DOC-Br Komplexe durch Eisenoxide immobilisiert. Die Fixierung von *I* und Br durch Eisenoxide scheint in diesen Böden eine wichtige Rolle zu spielen. Daraus lässt sich die Schlussfolgerung ziehen, dass tropische Böden mit hohen Gehalten an organischer Substanz und Eisenoxiden ein hohes Retentions- und Akkumulationspotenzial für *I* und Br aufweisen. Zudem erhalten sie einen hohen *I* und Br Eintrag durch hohe jährliche Niederschlagssummen.

## Acknowledgements

Special thanks goes to Prof. Harald Biester for enabling this project in Costa Rica, for supervising my master thesis and for an always open door concerning questions and problems. Furthermore, I thank Petra Schmidt and Adelina Calean for their tireless assistance and support in the preparation of sampling equipment and the laboratory analyses. A great thank you also goes to Dr. Christian Birkel who lent his support in the organisation and implementation of the field work and analyses at the university of Costa Rica and recommended the most delicious caribbean food stand to us. The staff of the Arturo Manuel Brenes Research Station made the stays in the study area very pleasant and provided us with delicious meals and the daily afternoon coffee. Particularly I'd also like to thank Laura Piechulla for having a great time in Costa Rica and Germany and for the good teamwork. Furthermore, I appreciate Apl. Prof. Rolf Nieder to have agreed on being the second supervisor of my master thesis and always having an open ear for soil related questions.

## 1 Introduction

### 1.1 Significance of iodine

Iodine (*I*) is a trace element and micronutrient in terrestrial ecosystems. Together with fluorine (F), chlorine (Cl) and bromine (Br) it forms the chemical group of halogens. It exists in multiple oxidation states and undergoes complex biogeochemical cycling, interacting with microorganisms, mineral- and organic phases. *I* plays a major role in regulating the metabolism in human cells through its involvement in the synthesis of thyroid hormones. Insufficient uptake can lead to iodine deficiency disorders (IDD). Goitre and cretinism are well known forms of IDD. (Andersson et al., 2007). *I* deficiency is especially dangerous in fetal state and was stated to be the greatest cause of preventable brain damage in childhood (Benoist, 2004).

Humans take up *I* through their nutrition. The recommended daily uptake for humans is 150 µg (Food and Nutrition Board, Institute of Medicine, 2006). Low *I* contents in soils due to past glaciation or intensive leaching processes by high rainfall lead to low *I* supply through food (Benoist, 2004). IDD are common in mountainous regions and also many tropical countries are concerned (Andersson et al., 2007; Dissanayake et al., 2007). Worldwide, one third of children in school-age is exposed to the risk of iodine deficiency (Benoist, 2004). The severe health effects lead to the fact that IDD represent a threat to social and economic development (Benoist, 2004). This points out the importance of understanding the behaviour of *I* in ecosystems.

An oversupply of *I* usually does not lead to measurable effects in humans, but can cause hyperfunction or dysfunction of the thyroid gland in some cases (Leung and Braverman, 2014). In plants, deficiency symptoms were not observed. However, plants play an important role for *I* fixation in terrestrial ecosystems (Fuge and Johnson, 1986). *I* toxicity effects in plants do not occur under natural conditions but were observed in contaminated areas and under paddy field conditions (Kabata-Pendias and Szteke, 2015).

### 1.2 Iodine cycling and -chemistry in soils

#### 1.2.1 The path of *I* from oceans to soils

An overview of the *I* cycle is given in Figure 1. The ocean provides the *I* source for soils. Almost 70 % of all crustal *I* is contained in ocean sediments and in continental sedimentary rocks (Muramatsu et al., 2004). The latter show a mean *I* concentration of 2 mg kg<sup>-1</sup> which is ten times the *I* content of igneous rocks (0.2 mg kg<sup>-1</sup>; Fuge and Johnson, 1986). In basalt it is even lower. Chai and Muramatsu (2007) measured a mean *I* concentration of less than 0.06 mg kg<sup>-1</sup> in four basalt reference materials. This can partly be attributed to the extreme rareness and instability of naturally occurring minerals containing *I* (Fuge and Johnson, 1986).

From the ocean, *I* volatilisation to the marine boundary layer occurs mainly in form of iodo-methane (CH<sub>3</sub>I), C<sub>3</sub>H<sub>7</sub>I, CH<sub>2</sub>I<sub>2</sub>, CH<sub>2</sub>ICl and CH<sub>2</sub>IBr (Gilfedder, 2008). *I* is transported in the

atmosphere in gaseous- or aerosol form and undergoes photochemical transformations (Saiz-Lopez et al., 2012).

*I* reaches soils, plants and surface waters by wet- and dry deposition, primarily in the form of soluble organic iodine (SOI) and to a lesser extent as iodate ( $\text{IO}_3^-$ ) and iodide (*I*) (Baker et al., 2001; Gilfedder et al., 2008). Plant uptake occurs through stomata from the atmosphere and in small amounts via roots from soil solution (Barry and Chamberlain, 1964; Whitehead, 1984). *I* deposited on leaves is washed from plants by rain. Incorporated *I* in plant tissues is passed to the soil with the decomposition of plant residues. Leached *I* from soils is transported almost exclusively in association with dissolved organic matter (DOM) to ground water (Xu et al., 2011b) and rivers (Moran et al., 2002), which lead it to other surface waters and finally back into the ocean.

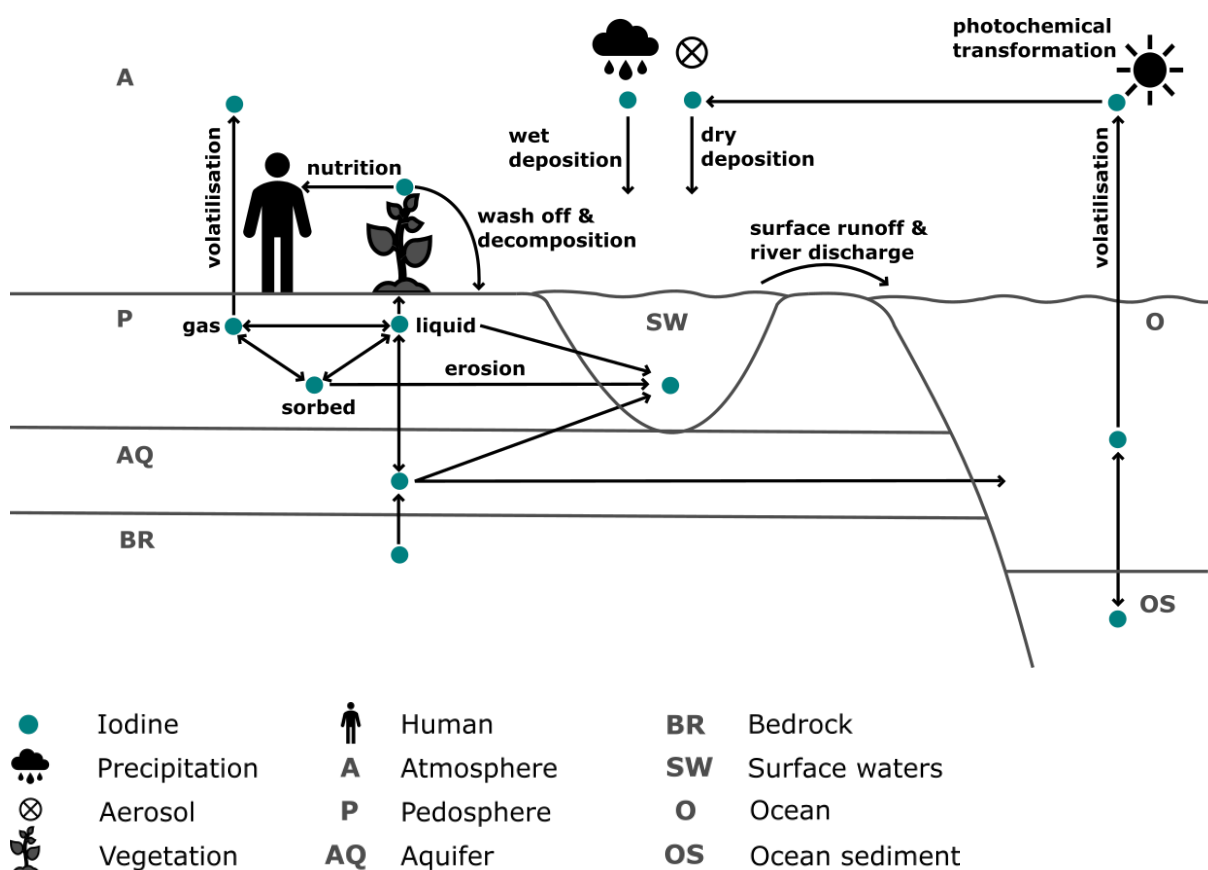


Figure 1: Overview of iodine cycling in the environment.

### 1.2.2 *I* sorption in soils

In soils, *I* can either be retained by sorption to the solid phase or mobilised through dissolution or adsorption to dissolved or colloidal particles. The iodine fixation potential (IFP) was introduced as a term to embrace the complex and interacting soil characteristics that determine *I* retention (Fuge and Johnson, 1986).

*I* soil chemistry is controlled by *I* speciation (Hu et al., 2005; Hu et al., 2009). Early studies reported that *I* sorption is predominantly influenced by redox conditions and pH (Yuita et al., 1991). More recent studies revealed that other soil environmental factors control *I* speciation and thereby *I* soil chemistry. The content of SOM (Xu et al., 2011b; Xu et al., 2011a), contents of clay minerals, abundance of sesquioxides (Shetaya et al., 2012; Yoshida et al., 1992), contact time with the soil matrix (Hu et al., 2009), microbial activity (Li et al., 2012b; Li et al., 2012a) and air temperature (Shetaya et al., 2012) were identified as the driving factors for *I* retention and mobility in soils.

The main dissolved inorganic *I* species under oxidising conditions was found to be  $\text{IO}_3^-$  (Yuita, 1992). But, organically bound forms are much more abundant (Emerson et al., 2014; Xu et al., 2011b; Yamada et al., 1999). OM was found to be the main binding partner for *I* in soils and therefore the dominant driver controlling *I* soil chemistry (Emerson et al., 2014; Santschi et al., 2017; Xu et al., 2011b; Xu et al., 2011a). Binding of *I* to OM occurs to aromatic, but also to aliphatic, OM structures through covalent bonding (Figure 2) and the substitution of a hydrogen (H) atom (Moulin et al., 2001; Stavber et al., 2008). Microorganisms play an important role for the halogenation of OM through the production of enzymes such as haloperoxidases. These catalyse the oxidation of halogens by hydrogen peroxide ( $\text{H}_2\text{O}_2$ ) (Butler and Sandy, 2009) and enable the halogen incorporation by microorganisms. Abiotic *I* oxidation was observed in the presence of manganese (Mn)- and iron (Fe) oxides (Allard and Gallard, 2013; Keppler et al., 2000). Reactive intermediates are formed during these processes, such as hypoiodous acid (HIO), and readily bound to OM or volatilised (Li et al., 2012b). Also, microbially released organic acids can promote *I* oxidation (Li et al., 2012b). The covalent bond between OM and *I* is highly stable (Moulin et al., 2001), whereas sorption to the mineral phase happens through weaker electrostatic adsorption (Hu et al., 2005).

SOM, clay minerals and sesquioxides provide complexation surfaces for *I* adsorption. pH values influence the charges of these surfaces. With increasing pH, the negative surface charges increase. Since *I* species are anionic, electrostatic repulsion increases with increasing pH (Allard and Gallard, 2013; Steinberg et al., 2008). Therefore, *I* sorption decreases with increasing pH (Whitehead, 1973).

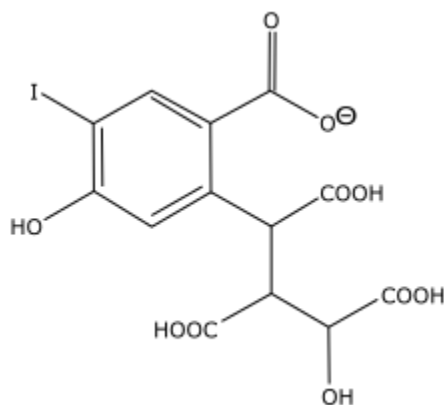


Figure 2: Iodine covalently bound to aromatic structure of fulvic acid (adapted from Moulin et al., 2001).

### 1.2.3 I mobility and volatilisation from soils

A major fraction of soluble *I* fractions exists as SOI, less abundant forms are  $\text{IO}_3^-$  or *I* (Emerson et al., 2014; Kaplan et al., 2014; Shetaya et al., 2012; Xu et al., 2011b; Yamada et al., 1999). A study from southern Germany showed that >80 % of riverine *I* transport takes place in form of SOI (Gilfedder et al., 2010). Therefore, its mobility in terrestrial environments is related to that of DOC (Xu et al., 2011b; Xu et al., 2011a) even in soils with low SOM and DOC contents (Santschi et al., 2017). Considerable amounts of *I* can also be mobilised as colloidal organically bound *I* (COI) (Xu et al., 2011b).

*I* volatilisation from soils occurs in form of  $\text{CH}_3\text{I}$ . This can be initiated biotically and abiotically (Allard and Gallard, 2013; Muramatsu et al., 2004). However, the global contribution of volatilised *I* from terrestrial sources remains unclear.

### **1.3 Tropical systems and volcanic soils**

#### **1.3.1 Characteristics of tropical forest ecosystems**

Tropical systems are highly physically structured ecosystems and therefore provide numerous microhabitats. These enable the high biodiversity of flora and fauna that the tropics are known for (Kricher, 2011). Continuously high temperatures (minimum air temperature  $\geq 18$  °C, Kottek et al., 2006) combined with high rainfall (minimum monthly precipitation  $\geq 60$  mm, Kottek et al., 2006) result in strong chemical weathering and leaching processes in soils (Zech et al., 2014). Also, tropical forest ecosystems are mostly old and therefore had abundant time for pedogenesis. This leads to highly weathered acidic soils with increased accumulation of Fe-Oxides (Zech et al., 2014). Ferralsols, plinthosols and Acrisols are typical soils in the tropics (Zech et al., 2014). Low nutrient status and fixation of essential elements require efficient nutrient uptake and use. This leads to fast nutrient recycling (Kricher, 2011; Vitousek, 1986). Due to warm and humid conditions, the biological activity in the soils is high. Therefore, plant residues are quickly decomposed by macro-fauna, bacteria and fungi, resulting in a rapid nutrient release and a thin litter layer. Distinct increases in soil microbial activity were observed following the onset of the rainy season (Cleveland et al., 2004).

#### **1.3.2 Tropical volcanic soils – Characteristics and pedogenesis**

In areas under the influence of volcanic activity, parent rock for soil development is younger due to the deposition of volcanic material during eruptions. Consequently, soils are less weathered. Andosol is a common soil type that forms on volcanic material (Nanzyo, 2002). Andosols are characterised by two dominant processes: First, the formation of amorphous minerals, such as allophanes or aluminium (Al)-Fe-humus complexes, and second the accumulation of OM (Gérard et al., 2007; Shoji et al., 1994). Other typical minerals in volcanic soils are imogolite and halloysite (Dahlgren et al., 2004).

Throughout soil development, primary minerals are physically and chemically weathered, leading to acidification, enrichment of Fe- and Al oxides, and a decrease in nutrient replenishment due to leaching of solution products (Ca, Na, Mg, K, Si). Silicon (Si) depletion and enrichment of Fe- and Al oxides are particularly pronounced in tropical soils owing to intensive weathering conditions (Scheffer et al., 2010).

Dahlgren et al. (2004) identified the following soil development series on volcanic material for warm, humid tropical regions: Leptosol – Andosol – Cambisol – Ferralsol (translated from USDA Soil Taxonomy to WRB). Also in a climosequence in Taiwan, Cambisols were found to develop from Andosols with preceding pedogenesis (Tsai et al., 2010).

## 1.4 Aims and hypotheses

Even though numerous previous studies investigated *I* soil chemistry, there is a lack of knowledge on soils of tropical ecosystems. High rainfall, humid and warm conditions, high Fe contents in soils and former volcanic activity constitute a special combination of factors influencing the fate of *I*. This demands a closer look at *I* soil chemistry in these systems.

This master thesis presents the results of an examination of *I* behaviour in nine soil profiles in a tropical, pristine pre-montane rainforest in Costa Rica. Solid soil samples and pore water samples will be taken. The water-soluble fraction will be assessed by batch leaching experiments. Furthermore, other main- and trace elements will be measured to reveal more information about *I* soil chemistry. Special interest will be placed on carbon (C), bromine (Br) and Fe. The results will be statistically analysed and related to soil properties.

The following questions will lead through the thesis: How much and which form of *I* is present in the investigated soils? How high is its mobility? What is the role of soil composition for *I* retention and mobilisation? What are the differences between *I* and Br soil chemistry? Are there relations between *I* and other elements? Which processes can explain the distribution and behaviour of *I*, Br and C?

Four hypotheses were defined: (1) Iodine is not leached out of the soil because it is adsorbed to OM and (2) Fe-Oxides. (3) DOC is degraded before it can be washed out of the soil. (4) *I*- and Br chemistry is similar in fixation and leaching processes in the soils of the ReBAMB.

The project also involves the master thesis of Laura Piechulla. She analysed rainwater, bedrock and river samples in the same study area and conducted a sequential extraction with solid soil samples. The results will be referred to in chapter 4.

## 2 Methods and study site

### 2.1 Study site

The study area is located in the Central Volcanic Cordillera in Costa Rica, Central America (Figure 3). It is part of the San Lorencito catchment, which comprises 3.2 km<sup>2</sup>, stretches from 890 to 1450 m of altitude and drains towards the Atlantic coast. The study area was formed five to nine million years ago in the tertiary-neogene by volcanic activity. The geology consists of basaltic and andesitic rocks. Steep v-valleys with a mean slope of 17° and highly dynamic rivers form the landscape. The vegetation represents a typical pre-montane forest and reaches a maximum height of about 50 m. The climate is characterised by an annual precipitation of 3.6 m, an annual potential evapotranspiration (PET) of 1.2 m, a mean annual air temperature of 21 °C and a relative humidity (RH) of 98 %. The dry season lasts from January until April and is followed by the rainy season (May-December). The study area belongs to the Antonio Manuel Brenes Biological Reserve (ReBAMB) and is managed by the University of Costa Rica. Its access is restricted to research only.

Two slopes, left (L) and right (R) slope, make up the study area and will be compared concerning soil characteristics, C, I and Br contents and mobility. The main difference between slope L and R is the maximum inclination with 68° and 63° respectively. Also, the terrain surface on slope L is clearly rougher and more irregular, while it is rather even on slope R.

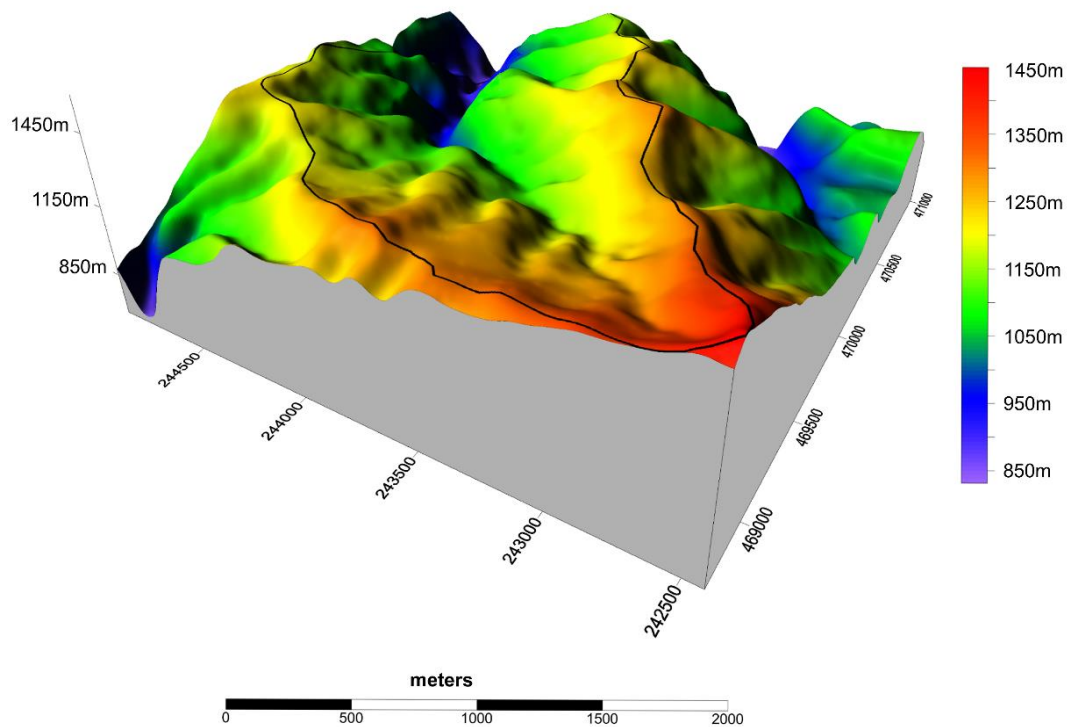


Figure 3: Location and digital elevation model of the study area, ReBAMB, Costa Rica.

## 2.2 Sampling sites, field parameters and sampling technique

Soil samples were taken from nine soil profiles on the slopes L and R (Figure 4) on four days in June 2017, in the beginning of the rainy season. The sites for the profiles were evenly distributed over the two slopes. In the middle of each slope, one soil profile with a depth of approximately 1x0.7 m was established (L2 and R2). To take spatial variations of the measured parameters into account, seven shallower soil profiles, approximately 0.5x0.7 m (L1, L3, L4, R1, R3, R4, R5), were sampled.

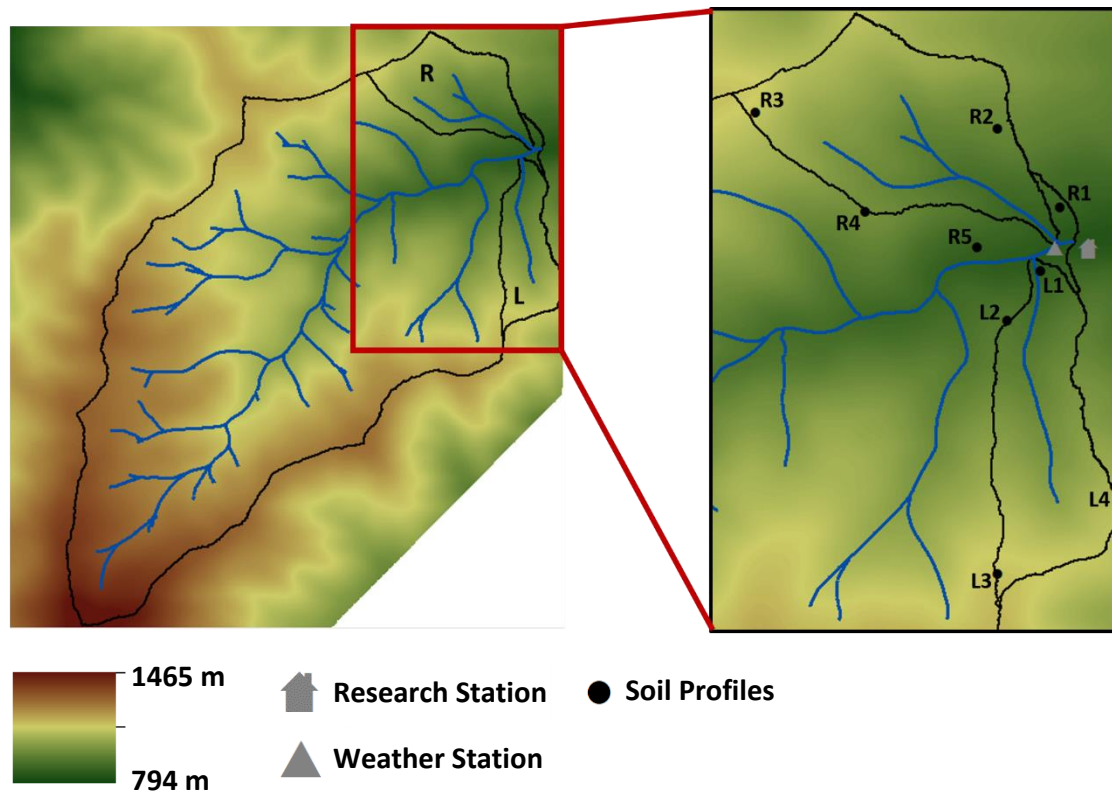


Figure 4: Left: Overview of the San Lorencito catchment, ReBAMB, Costa Rica; Right: location of soil profiles on slope L and R, research station (house) and weather station (triangle).

### 2.2.1 Solid soil samples

At each soil profile 0.5 kg of disturbed soil material was taken from the middle of each horizon and stored in plastic bags (Whirl Packs). The sampling was conducted by hand, wearing gloves to prevent sample contamination. The soil depth was assessed by using a manual soil drill. Data on thickness of the organic layer, aggregate type, Munsell colour, rooting, soil depth, skeleton (>2 mm) percentage, texture, pore volume and activity of macrofauna, was recorded in the field following KA5 standards (Eckelmann et al., 2006). Soil types were defined using the World Reference Base for Soil Resources (WRB).

## 2.2.2 Soil pore water sampling

To extract pore water, rhizones were installed at profiles L2 and R2 in the middle of each soil horizon. At profiles L1 and R5, pore water was extracted by installing a Prenart Super Quartz suction tube in the top- and subsoil (5 cm and 25 cm). Pore water was extracted by vacuum for 24 hours.

Solid samples were kept at 4 °C, pore water samples were frozen (-18 °C). All samples were shipped to Germany for analysis. A summary of sample preparation and analysis methods is given in Figure 5.

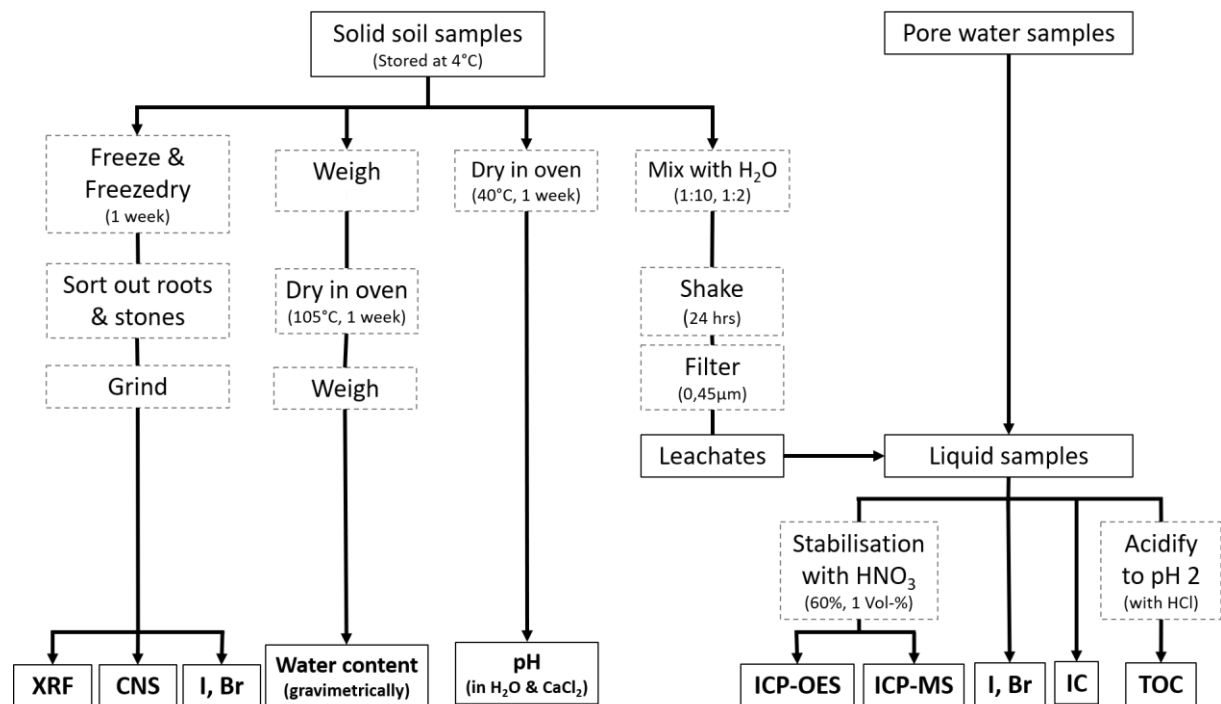


Figure 5: Summary of sample preparation and analytical methods for solid soil samples, soil pore water and leachates.

## 2.3 pH value, water content and texture

The pH value of air-dried soil was measured in water and 0.01 M calcium chloride ( $\text{CaCl}_2$ ) solution (modified after DIN 19684-1) with a soil-liquid ratio of 1:2.5. Measurement of pH in 0.01 M  $\text{CaCl}_2$  is less sensitive to the soil electrical conductivity (EC) than the pH measurement in water. The addition of 0.01 M  $\text{CaCl}_2$  to the solution leads to the exchange of  $\text{Ca}^+$  with  $\text{H}^+$  and  $\text{Al}^+$  at sorption sites of solid soil. This results in a lower pH when measured in 0.01 M  $\text{CaCl}_2$  than the one measured in water (Miller and Kissel, 2010). Differences between the two methods decrease with increasing EC (Minasny et al., 2011). Both methods are commonly used.

The water content ( $\theta$ ) was determined gravimetrically for the horizons of profiles L2 and R2. It was calculated with the weight of the wet ( $s_w$ ) and the oven dry soil ( $s_d$ ):

$$\theta = \frac{s_w - s_d}{s_d}$$

*EQ 1: Calculation of gravimetric water content ( $\theta$ )*

The soil texture was determined by hand texturing. Samples of profiles L2 and R2 were analysed by Roland Prietz (Thünen Institute of Climate-smart Agriculture, Braunschweig). Hand texturing by experienced scientists, was shown to be an appropriate alternative to laboratory texture analysis (Vos et al., 2016). All other samples were analysed in the field.

## 2.4 Soil characterisation

General soil properties can be found in Table 1. The bedrock horizon (C\*) was not found in any of the profiles. The volcanic origin of the soils was evidenced by volcanic bedrock (basalt, andesite) and ash layers. The humus form and C/N ratios (median topsoil: 12) indicated fast decomposition (Blum, 2012; Scheffer et al., 2010). Skeleton was rare, fine roots were abundant in Ah, while coarse rooting intensity was higher in Bw horizons. The soils show high porosity allowing fast infiltration of rainwater. The ground vegetation was dense.

*Table 1: General soil properties of all soil profiles on slopes L and R, assessed according to the German soil classification KA5 (Eckelmann et al., 2006).*

<i>General Properties</i>	
Depth	>1.50 m
Humus form	Mull
Skeleton (>2 mm)	< 10 %
Rooting intensity	High, coarse & fine roots
Rooting depth	> 70 cm
Bulk density	Very low – low
Pores	Abundance: medium – high Size: fine – medium
Earthworm activity	1-10 individuals per m <sup>2</sup>

On slope L, three out of four soil profiles were Colluvic Cambisols and one is a Haplic Cambisol (Table 2). High C contents in AhBw horizons of profiles L1, L3 and L4 suggested it to be eroded topsoil material. The texture was clayey silt with an increase of clay content with depth (texture range: Ut2 – Uls – Tu3). The aggregates were stable and turned from crumbs in topsoil horizons into subpolyeders in subsoils. Munsell soil colours varied between 10YR-2/1 and 10YR-3/4. Soil profile L3 is shown as an example for a Colluvic Cambisol in Figure 6. Soil profiles L1, L2 and L4 are shown in Appendix 1 and Appendix 2.

The soil characteristics of soil profiles on slope R are shown in Table 3. All profiles are Haplic or Dystric Cambisols and do not seem to have been interrupted in their development through major erosion events. C contents are similar among all profiles. Aggregate types are crumbs in

topsoils and subpolyeders in subsoils. Texture varied from Ut2 over Slu to Tu3 and Munsell soil colours between 10YR-2/1 and 10YR-3/4. As an example for a Haplic Cambisol, Figure 7 shows the soil profile R2. Soil profiles R1 and R3-R5 are shown in Appendix 3 to Appendix 5.

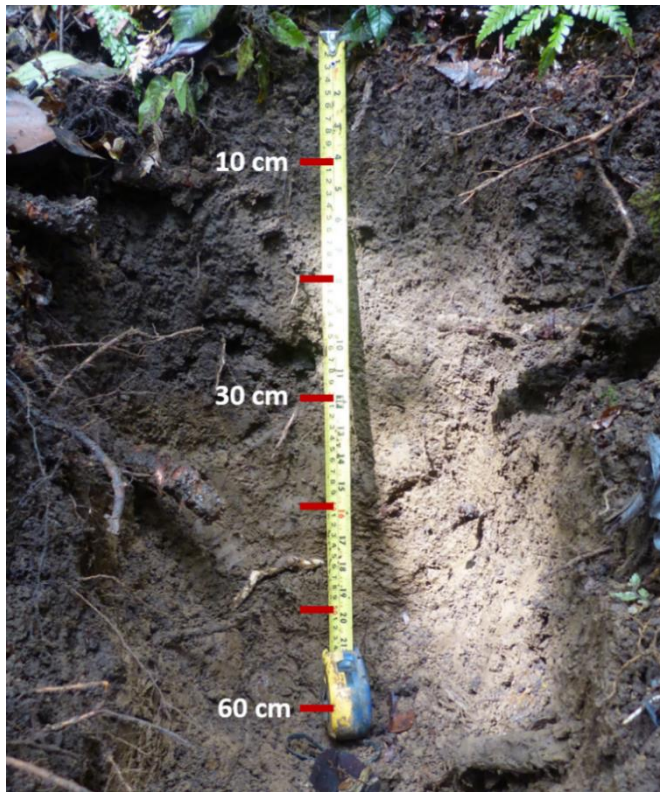


*Figure 6: Soil profile L3, Colluvic Cambisol, ReBAMB, Costa Rica, June 2017.*

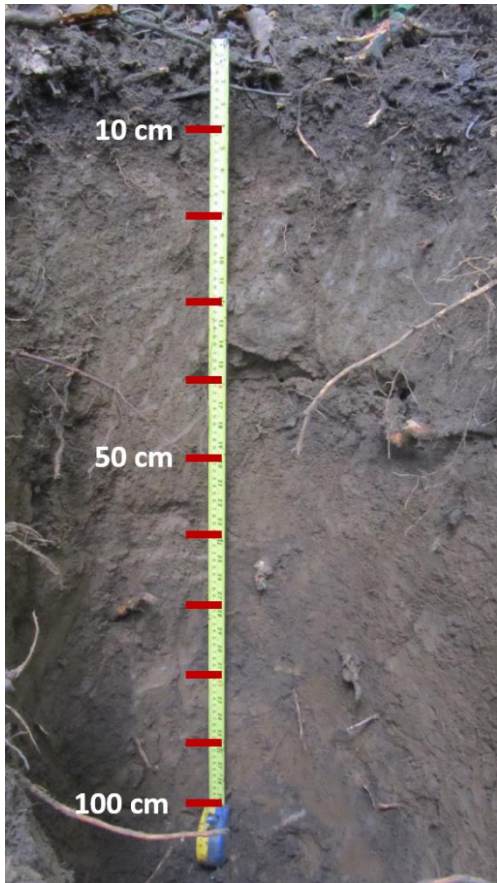


Figure 7: Soil profile R2, Haplic Cambisol, ReBAMB, Costa Rica, June 2017.

In the subsequent chapters, Ah horizons will be referred to as topsoil horizons, AhBw as transitional horizons and Bw as subsoil horizons. Given depths represent sampling depths. If all profiles are addressed, for topsoil horizons this will be 5-6 cm and for transitional soil horizons 15-20 cm. Subsoil horizons will be marked as depths  $\geq 30$  cm, even if the sampling of the subsoil horizon in profile R3 occurred in 20 cm depth.

pH values and gravimetric water content were only determined for profiles L2, R2 and R4 (Table 4).  $\text{pH}_{\text{H}_2\text{O}}$  values vary between 4.4 and 5.6. The pH value of profile R4 was more acidic than in profiles L2 and R2. Also,  $\text{pH}_{\text{H}_2\text{O}}$  and  $\text{pH}_{\text{CaCl}_2}$  values were very similar in profile R4. This can be attributed to the lower pH values and a possibly higher electrical conductivity in the soil solution (Minasny et al., 2011). The mean water content was 14 %. The high porosity of the soils might be a remnant of former Andosols, that have now weathered and turned into Cambisols.

Table 2: Soil characteristics of profiles on slope L, assessed according to German classification KA5 (Eckelmann et al., 2006) and WRB soil types.

<i>Profile</i>	<i>Horizon symbol</i>	<i>Depth [cm]</i>	<i>Texture</i>	<i>C [g kg<sup>-1</sup>]</i>	<i>C/N [-]</i>	<i>Aggr. type**</i>	<i>Munsell colour</i>
<b>L1</b>							
Colluvic							
Cambisol	Ah	0-10	Ut2	112	10	cru	10YR-2/2
	AhBw	> 10	Ut3	58	16	cru/sub	10YR-3/4
<b>L2</b>							
Haplic							
Cambisol	Ah	0-12	Ut3*	338	17	cru	10YR-2/2
	AhBw	12-30	Ut3*	119	12	cru	10YR-3/2
	Bw1	30-70	Ut4*	30	7	cru/sub	10YR-3/4
	Bw2	> 70	Lu*	16	7	sub	10YR-3/4
<b>L3</b>							
Colluvic							
Cambisol	Ah	0-7	Ut4	192	14	cru	10YR-2/1
	AhBw	7-26	Ut4	117	12	cru/sub	10YR-2/2
	II Bw	> 26	Tu3	23	6	sub	10YR-4/3
<b>L4</b>							
Colluvic							
Cambisol	Ah	0-10	Uls	187	12	cru	10YR-2/1
	AhBw	10-35	Ut3	60	9	cru	10YR-2/2
	II Bw	> 35	Ut4	42	7	sub	10YR-3/4

\* analysed by Roland Prietz

\*\* cru = crumbs; sub = subpolyeder

Table 3: Soil characteristics of profiles on slope R, assessed according to German classification KA5 (Eckelmann et al., 2006) and WRB soil types.

Profile	Horizon symbol	Depth [cm]	Texture	C [g kg <sup>-1</sup> ]	C/N	Aggr. Type***	Munsell Colour
<b>R1</b>							
Cambisol	Ah	0-8	Slu	129	12	cru	-
	Bw	>8	Slu*	33	7	sub	-
<b>R2</b>							
Haplic							
Cambisol	Ah	0-10	Ut3**	100	11	cru	10YR-2/1
	AhBw	10-30	Ut3**	64	9	cru	10YR-2/2
	Bw	> 30	Ut4**	25	6	sub	10YR-3/4
<b>R3</b>							
Cambisol	Ah	0-13	Ut2	112	12	cru	10YR-2/2
	Bw1	13-32	Lu	47	8	sub	10YR-3/4
	Bw2	>32	Lu/Tu3	27	6	sub	10YR-3/4
<b>R4</b>							
Dystric							
Cambisol	Ah	0-15	Ut3	132	12	cru	10YR-2/2
	Bw	>15	Lu	29	7	sub	10YR-3/4
<b>R5</b>							
Cambisol	Ah	0-8	Uls	109	11	cru	10YR-2/2
	Bw	>8	Lu	42	7	sub	10YR-3/4

\* more silt and clay than in overlying soil horizon

\*\* analysed by Roland Prietz

\*\*\* cru = crumbs; sub = subpolyeder

Table 4: pH values in water ( $pH_{H_2O}$ ) and 0.01 M calcium chloride ( $pH_{CaCl_2}$ ) solution and gravimetric water content of profiles L2, R2 and R4.

Soil profile	Horizon symbol	$pH_{H_2O}$	$pH_{CaCl_2}$	Water content [%]
<b>L2</b>				
Cambisol	Ah	4.8	4.1	18
	AhBw	5.5	4.6	14
	Bw1	5.6	4.9	13
	Bw2	5.3	4.4	11
<b>R2</b>				
Cambisol	Ah	5.0	4.7	14
	AhBw	5.3	4.8	14
	Bw	5.4	4.4	13
<b>R4</b>				
Dystric Cambisol	Ah	4.6	4.3	-
	Bw	4.4	4.4	-

## 2.5 Chemical analysis

The solid soil samples were dried in the freeze dryer (LYOVAC GT 2-E) for one week and ground. C, N and S contents were measured in an elemental analyser (EuroEA 3000), random triplicates were included. The detection limits for this method were  $3 \mu\text{g kg}^{-1}$  for C and  $1 \mu\text{g kg}^{-1}$  for N and S. A major and trace elemental screening was conducted by means of XRF according to the method used by Cheburkin and Shotyk (1996) using triplicates, the detection limit for Fe was 0.0001 %.

I- and Br analyses were carried out by thermal extraction, trapping the I and Br in water followed by ICP-MS-analyses. The detection limit for I and Br was  $0.3 \mu\text{g L}^{-1}$  and  $0.4 \mu\text{g L}^{-1}$  respectively.

The porewater samples were defrosted over night at room temperature and analysed by means of ICP-MS (Agilent 7700), ICP-OES (Varian 715-ES) and IC (761 Compact IC). For ICP-MS and ICP-OES the samples were stabilized with 1 Vol-% of nitric acid ( $\text{HNO}_3$ , 60 %). The pore water sample from the Ah horizon of profile R2 did not provide enough fluid for the ICP-MS analyses and was therefore diluted with water (1:1.5625). I and Br were determined in ICP-MS with untreated porewater samples. For IC the untreated samples were processed.

Also, the content of dissolved organic carbon (DOC) was determined by means of thermal desorption in a TOC-Analyser (multi N/C 2100). Inorganic C was eliminated before the measurement by acidifying the fluid with hydrochloric acid (HCl, 37 %) and adjusting the pH to 2.

With this data, the I, Br, C and Fe status of the soils in the ReBAMB will be assessed. Subsequently, the determining processes for I and Br accumulation will be identified. The soil chemistry of I and Br will be compared by the calculation of I/Br ratios.

## 2.6 Batch leaching experiments

To evaluate the total leachable amounts of I, Br, DOC and other main- and trace elements in the soil samples, batch leaching experiments were conducted. An aliquot sample of 10 g of fresh soil was mixed with 100 ml of water, shaken for 24 hours and filtered with a 0.45 µm membrane nylon filter. The leachates were analysed in the same way as the pore water samples. Because the results from leachate analyses provide a higher comparability, only these were used for statistical analysis. A comparison of element concentrations in leachates and pore water samples will be provided in chapter 4.2.12.

## 2.7 Statistical analysis

Statistical analysis was conducted using Microsoft Excel 2016 and R Studio (Version 1.0.136). For the illustration and geographical analysis of the study area ArcGIS 10.5 was applied.

To obtain the percentage of the leachable fraction, I, Br and C contents in solid soil samples were calculated for dry soil with the mean water content (14 %). The ratio was calculated as follows:

$$f_{x, leach} = \frac{m_{x, leach}}{m_{x, tot}} \quad EQ 2: \text{Calculation of leachable element fractions [\%]}$$

- $f_{x, leach}$  = Percentage of leachable fraction from total content of element x
- $m_{x, leach}$  = Mass of element x in leachate
- $m_{x, tot}$  = Mass of element in dry solid sample

The spearman correlation coefficient ( $\rho$ ) was used to identify correlations between I, Br, C and DOC. To prevent two-point correlations, horizons with high values of I, Br and DOC were excluded (L1 Ah, L2 Ah and R4 Ah). For values showing large variations, the median instead of the arithmetic mean was calculated.

## 3 Results

### 3.1 Solid soil samples

#### 3.1.1 *I* and *Br* concentrations in solid samples

*I* concentration in solid samples ranged from 52.7 mg kg<sup>-1</sup> (R2 Bw, 65 cm) to 129.6 mg kg<sup>-1</sup> (L2 AhBw, 20 cm; Figure 8). Highest values in solid samples were found in depths ≤20 cm for six out of nine profiles (L2, L3, L4, R2, R3, R4). Exceptions were profiles L1 and R1 where subsoil horizons (L1: 20 cm, R1: 40 cm) showed a slightly higher *I* content than topsoils (5 cm). Soil profile R5 did only show a small change in concentration with depth (0.13 mg kg<sup>-1</sup>). In seven out of nine profiles, the topsoil horizons (5-6 cm) showed lower *I* concentrations than the horizon below. Exceptions were profiles L4 and R4. The variation of *I* concentrations with depth in solid samples was low with a median of 23.4 mg kg<sup>-1</sup> accounting for 34 % of the median *I* concentration in solid samples.

The range for *Br* concentrations in solid samples was 43.7 mg kg<sup>-1</sup> (R2 Bw, 65 cm) to 165.3 mg kg<sup>-1</sup> (L2 AhBw, 20 cm; Figure 8). *Br* maxima were found in depths ≤20 cm in six out of nine soil profiles (L2, L3, L4, R2, R3, R4). Profiles L1, R1 and R5 constituted exceptions since *Br* concentrations were slightly higher in subsoils.

*Br* concentrations in solid samples of topsoils (5-6 cm) and transitional horizons (15-20 cm) of slope L were higher than *I* concentrations (Figure 8). On slope R, this was only true for three out of five profiles (R3-R5). *Br* concentrations of solid samples in profile R1 were slightly lower than *I* concentrations. Profile R2 showed only a deviation of 1-2 % of *Br* from *I* concentrations in topsoil (5 cm) and the transitional horizon (15 cm). The median difference between *I* and *Br* concentrations was larger on slope L than on slope R with 10.4 mg kg<sup>-1</sup> and 7.4 mg kg<sup>-1</sup>, respectively. Patterns in depth profiles of *I* and *Br* solid sample concentrations were different among the profiles but similar for the two elements.

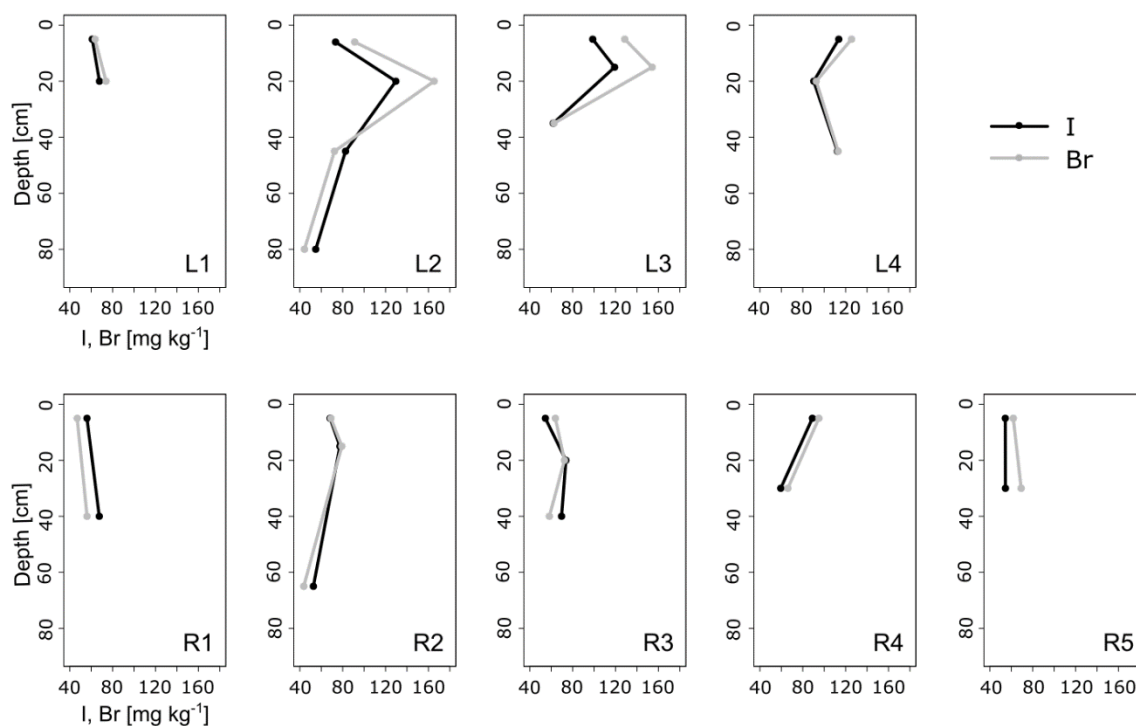


Figure 8: Iodine (I) and bromine (Br) concentrations in solid soil samples [ $\text{mg kg}^{-1}$ ] of profiles L1-L4 and R1-R5, shown at the average depth for each sampled horizon (Table 2 and Table 3).

### 3.1.2 C and Fe concentrations in solid samples

Solid sample C concentrations ranged from  $16.3 \text{ g kg}^{-1}$  (L2 Bw2, 80 cm) to  $337.8 \text{ g kg}^{-1}$  (L2 Ah, 6 cm; Figure 9). In profile L2 the C content in the topsoil horizon was above 30 %. Because of its low thickness it was nevertheless characterised as a mineral horizon with peaty characteristics instead of an organic horizon. This should be considered for the comparison to the other topsoil horizons. Therefore, second highest values are given, when useful. The second highest C concentration was  $191.5 \text{ g kg}^{-1}$  (L3 Ah, 5 cm), and the median was  $62 \text{ g kg}^{-1}$ . Maxima of C concentrations were measured in topsoil horizons (5-6 cm) in all profiles and minima in subsoil horizons ( $\geq 30$  cm).

The range of Fe concentrations in solid samples was  $42.7 \text{ g kg}^{-1}$  (L2 Ah, 6 cm) to  $175.8 \text{ g kg}^{-1}$  (L3 Bw, 35 cm; Figure 10). Fe concentrations were highest in subsoil horizons, except for profiles L1 and R5, where Fe concentrations were slightly higher in topsoil horizons (5 cm). But it has to be considered, that L1 and R5 were shallow and might show higher Fe concentrations in greater depths.

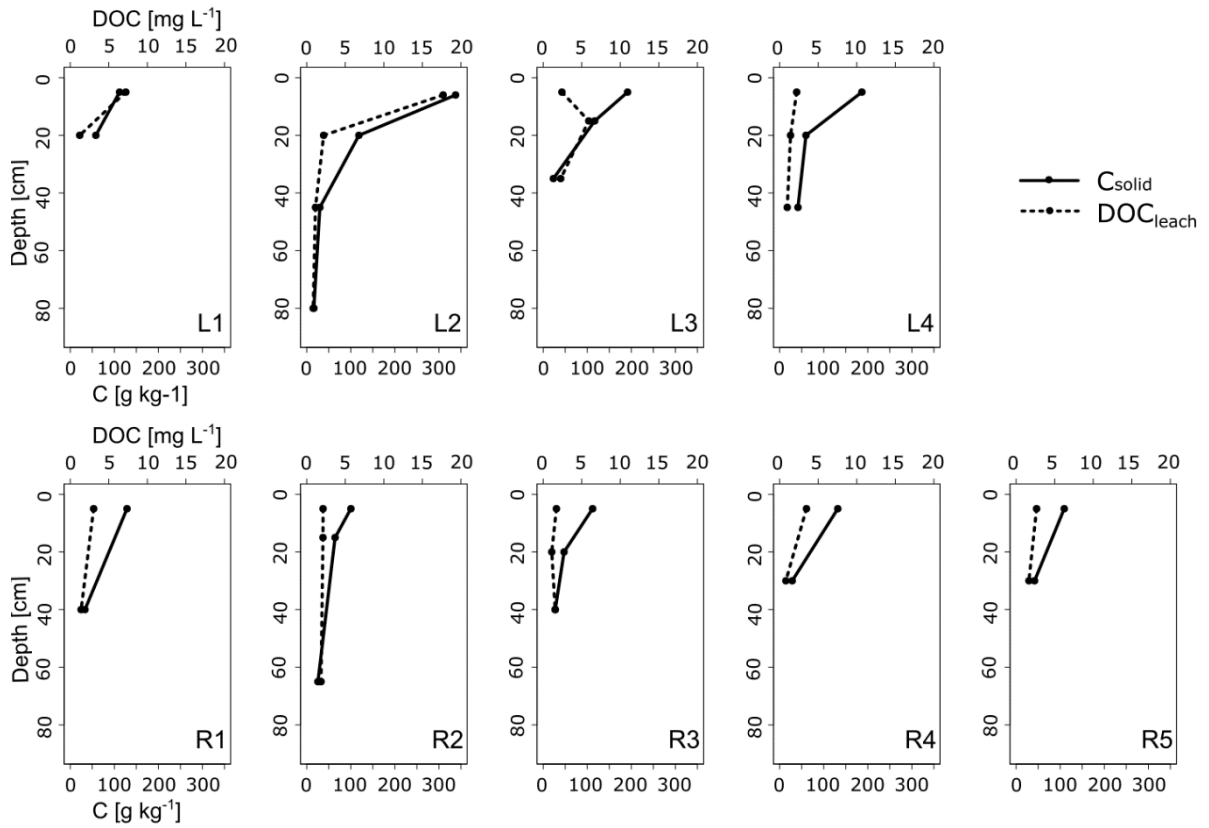


Figure 9: Carbon (C) concentrations in solid samples [ $\text{mg kg}^{-1}$ ] and leachates [ $\text{mg L}^{-1}$ ] in profiles L1-L4 and R1-R5, shown at the average depth for each sampled horizon (Table 2 and Table 3).

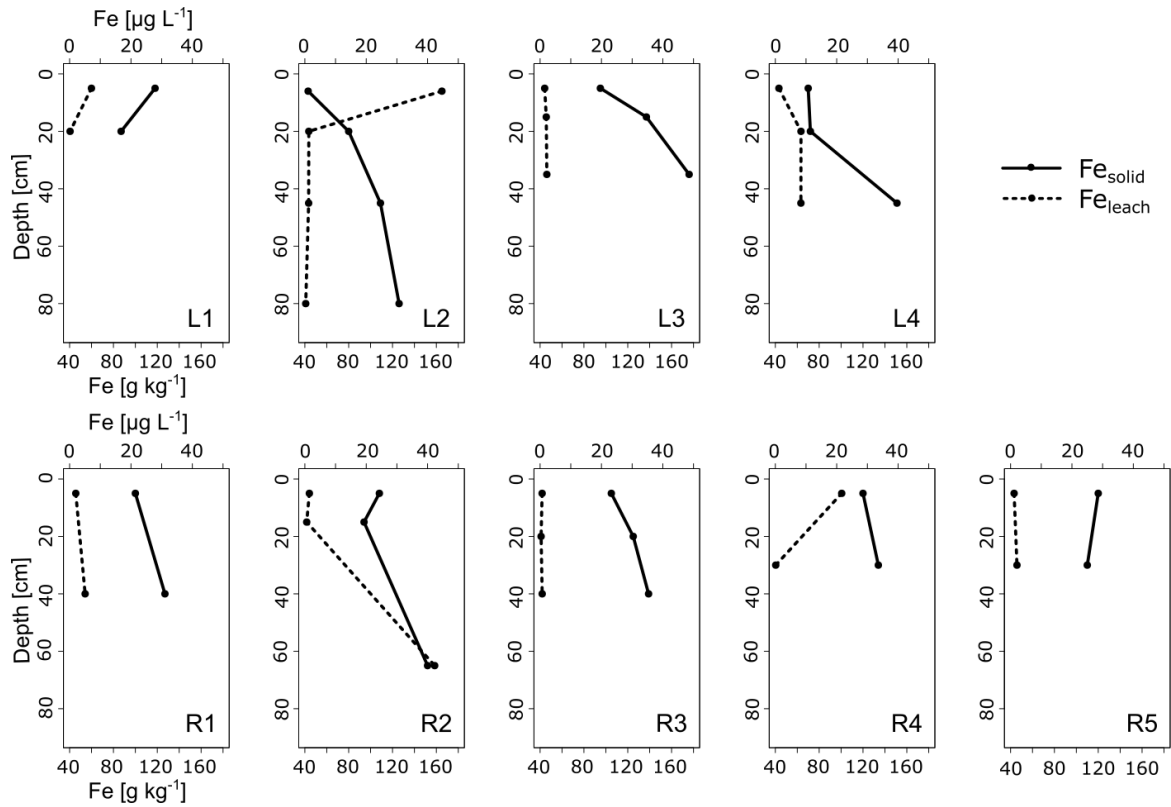


Figure 10: Iron (Fe) concentrations in solid samples [ $\text{g kg}^{-1}$ ] and leachates [ $\mu\text{g L}^{-1}$ ] in profiles L1-L4 and R1-R5, shown at the average depth for each sampled horizon (Table 2 and Table 3).

### 3.1.3 Quality of solid soil sample analyses

The quality of solid soil analyses was controlled by the analysis of certified reference materials (Table 5). Despite small deviations of measured values from certified values of *I* in the China Soil reference, C and N in the MOC reference and Fe in the LKSD4 reference, the measurement quality was adequate. Deviations from certified values in CNS and XRF measurements were higher, but the accuracy of the measurements was still satisfactory for the desired interpretation.

Table 5: Reference materials for solid soil analyses with certified values (CV) and measured values (MV).

<i>Technique</i>	<i>Reference</i>	<i>No.</i>	<i>Element</i>	<i>Unit</i>	<i>CV</i>	<i>MV</i>
Thermal extr. & ICP-MS	China Sediment	NCS DC 73312	<i>I</i>	mg kg <sup>-1</sup>	2.9 ± 0.4	2.79
			Br	mg kg <sup>-1</sup>	3.0 ± 0.6	2.68
	China Soil	DC 73030	<i>I</i>	mg kg <sup>-1</sup>	9.4 ± 1.1	7.00
			Br	mg kg <sup>-1</sup>	4.0 ± 0.7	4.54
CNS	China Sediment	NCS DC 73312	C	g kg <sup>-1</sup>	4.2	4.28
	MOC	115255	C	g kg <sup>-1</sup>	31.9 ± 0.7	34.96
			N	g kg <sup>-1</sup>	2.7 ± 0.2	5.09
XRF	LKSD4	-	Fe	g kg <sup>-1</sup>	28.68	3
			Cl	g kg <sup>-1</sup>	-	194
			Mn	mg kg <sup>-1</sup>	774	500
			Ni	mg kg <sup>-1</sup>	31 ± 5	27
			Cu	mg kg <sup>-1</sup>	31 ± 4	22
			As	mg kg <sup>-1</sup>	16 ± 1	14
			Rb	mg kg <sup>-1</sup>	28 ± 10	27
			Sr	mg kg <sup>-1</sup>	110 ± 38	115
			Y	mg kg <sup>-1</sup>	23 ± 10	20
			Zr	mg kg <sup>-1</sup>	105 ± 17	78
			Pb	mg kg <sup>-1</sup>	91 ± 6	86
			Si	g kg <sup>-1</sup>	194	162
			DMA	LKSD4	-	Hg

## 3.2 Leachates

### 3.2.1 *I* and Br concentrations in leachates

The minimum *I* concentration in leachates was  $0.2 \mu\text{g L}^{-1}$  (R5 Bw, 30 cm), the maximum  $21.9 \mu\text{g L}^{-1}$  (L2 Ah, 6 cm) and the median  $0.9 \mu\text{g L}^{-1}$  (Figure 11). Highest *I* concentrations of leachates from the respective soil profiles were found in depths  $\leq 20$  cm, except for profile R2, where the highest *I* content was in the Bw horizon (65 cm). In leachates, median variations of *I* concentrations between top- and subsoil were big and comprised  $0.9 \mu\text{g L}^{-1}$ . This corresponds to 100 % of the median leachate *I* concentration.

Despite high *I* content in solid samples, the maximum water leachable fraction was only 0.4 % (L2 Ah, 6 cm; Figure 12). The second highest percentage of leachable *I* was 0.2 % in the Ah horizon of profile R4. The median percentage of leachable *I* was 0.01 %.

Br concentrations ranged from  $0.4 \mu\text{g L}^{-1}$  (L2 Bw2, 80 cm) to  $47.0 \mu\text{g L}^{-1}$  (L2 Ah, 6 cm) and the median was  $3.2 \mu\text{g L}^{-1}$  (Figure 11). In all soil profiles, highest concentrations were found in topsoils (5-6 cm). The median leachable fraction of Br comprised 0.04 % and a maximum of 0.6 % (L2 Ah, 6 cm; Figure 12). The second highest leachable percentage was 0.2 % (L1 Ah, 5 cm).

Leachable Br concentrations were higher than leachable *I* concentrations in topsoils (5-6 cm) and transitional horizons (15-20 cm), except for profile R4 (Figure 11). Differences in *I* and Br concentrations in leachates of slope L were higher than on slope R, with  $5.5 \mu\text{g L}^{-1}$  and  $2.0 \mu\text{g L}^{-1}$ , respectively.

For both, *I* and Br, maximum leachable fractions were in topsoils (5-6 cm) and minima in subsoils ( $\geq 30$  cm; Figure 12). Except for L3 and R2 where percentages of leached *I* fractions were slightly higher in Bw horizons ( $\geq 35$  cm). Overall, percentages of leached *I* and Br fractions were low. Depth patterns of leached *I* and Br percentages were similar for the two elements, with in most cases higher values for Br.

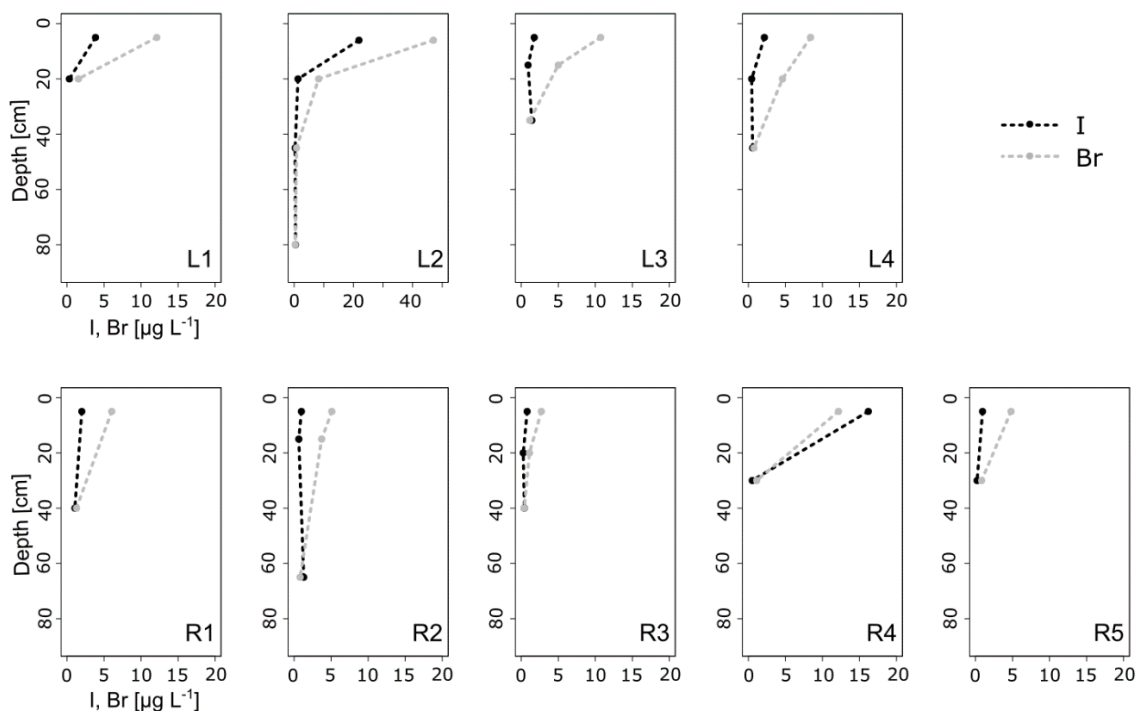


Figure 11: Iodine (I) and Bromine (Br) concentrations in leachates [ $\mu\text{g L}^{-1}$ ] of profiles L1-L4 and R1-R5, shown at the average depth for each sampled horizon (Table 2 and Table 3), with x-axis scale set to 50 for L2.

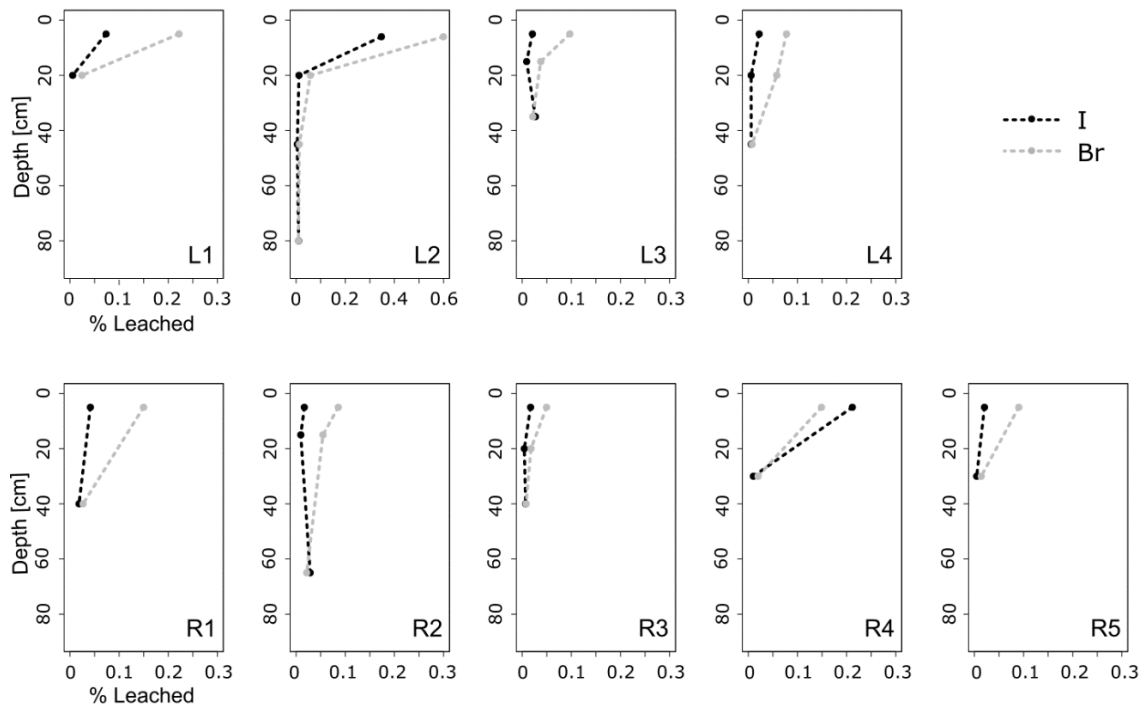


Figure 12: Percentage of leachable fraction of I and Br, calculated for dry soil samples of profiles L1-4 and R1-5, shown at the average depth for each sampled horizon (Table 2 and Table 3), with x-axis scale set to 0.6 % for L2.

### 3.2.2 DOC and Fe concentrations in leachates

The maximum DOC value in soil leachates was  $17.7 \text{ mg L}^{-1}$  (L2 Ah, 6 cm), the minimum  $0.8 \text{ mg L}^{-1}$  (R4 Bw, 30 cm) and the median  $2.0 \text{ mg L}^{-1}$  (Figure 9). In leachate samples the highest DOC concentrations were measured in topsoil horizons (5-6 cm). Except for leachates of profile L3, where highest DOC values were measured in the transitional horizon (15 cm).

The maximum leachable DOC proportion was only 0.1 %, despite high C contents in solid samples.

Leachate Fe concentrations ranged from  $0.1 \text{ } \mu\text{g L}^{-1}$  (R4 Bw, 30 cm) to  $44.7 \text{ } \mu\text{g L}^{-1}$  (L2 Ah, 6 cm), the median was  $1.5 \text{ } \mu\text{g L}^{-1}$  (Figure 10). Depth profiles of leached Fe concentrations did not show consistent patterns. Three profiles showed maximum concentrations in topsoils (L1, L2, R4), one in the transitional horizon (L4), two in subsoils (R1, R2) and three showed only a mean variation with depth of  $0.7 \text{ mg L}^{-1}$  (L3, R3, R5).

### 3.2.3 Quality of leachates and pore water analyses

The quality of leachate and pore water analyses was controlled by the analysis of certified reference materials (Table 6). IC measurements, DOC, Y, La and U analyses showed small deviations from certified values, but these do not influence conclusions drawn from the results.

Table 6: Reference materials for liquid sample analyses with certified values (CV) and measured values (MV) for leachates (MV 1) and pore water samples (MV 2).

<i>Tech-nique</i>	<i>Reference/Standard</i>	<i>No.</i>	<i>Element</i>	<i>Unit</i>	<i>CV</i>	<i>MV 1</i>	<i>MV 2</i>
ICP-MS	Roth	-	I	$\mu\text{g L}^{-1}$	5	5.21	5.21
			Br	$\mu\text{g L}^{-1}$	5	5.17	5.28
	Fluka Kontroll	54704	I	$\mu\text{g L}^{-1}$	10	10.03	10.13
			Br	$\mu\text{g L}^{-1}$	10	10.14	10.41
	River Thames	LGC6019	Fe	$\mu\text{g L}^{-1}$	$287 \pm 7$	289.57	288.39
			Al	$\mu\text{g L}^{-1}$	$73 \pm 13$	77	85
	SPS-SW1	-	Pb	$\mu\text{g L}^{-1}$	$5.2 \pm 0.3$	5	5
			As	$\mu\text{g L}^{-1}$	$10.0 \pm 0.1$	10	10
	River Thames	LGC6019	Y	$\mu\text{g L}^{-1}$	$0.5 \pm 0.01$	0.1	0.1
			La	$\mu\text{g L}^{-1}$	$0.5 \pm 0.01$	0.5	0.4
	River Thames	LGC6019	Ce	$\mu\text{g L}^{-1}$	$0.5 \pm 0.01$	0.5	0.5
			U	$\mu\text{g L}^{-1}$	$0.5 \pm 0.01$	0.3	0.4
ICP-OES	River Thames	LGC6019	Mg	$\text{mg L}^{-1}$	$4.62 \pm 0.12$	4.56	4.55
			Ca	$\text{mg L}^{-1}$	$109 \pm 3$	107.92	107.49
			Mn	$\mu\text{g L}^{-1}$	-	23.73	23.70

IC	Roth	-	Cl <sup>-</sup>	mg L <sup>-1</sup>	10.040 ± 0.039	9.98	9.56
			NO <sub>3</sub> <sup>-</sup>	mg L <sup>-1</sup>	25.247 ± 0.103	24.44	22.48
			SO <sub>4</sub> <sup>2-</sup>	mg L <sup>-1</sup>	30.175 ± 0.110	27.35	26.29
TOC	TOC20	-	DOC	mg L <sup>-1</sup>	20	21.14	21.31
	Mauri Water	MAURI-09	DOC	mg L <sup>-1</sup>	5.92 ± 0.77	7.14	-

### 3.3 Correlations

#### 3.3.1 Correlations of I and Br with C and DOC

I and Br showed a weak correlation with C in solid samples (*I*-C: 0.42; Br-C: 0.57) and a stronger correlation with DOC in leachates (*I*-DOC: 0.7; Br-DOC: 0.74; Figure 13). The correlation of C was stronger for Br in solid samples and stronger for *I* in leachates. Therefore, *I* and Br chemistry in leachates is linked to C.

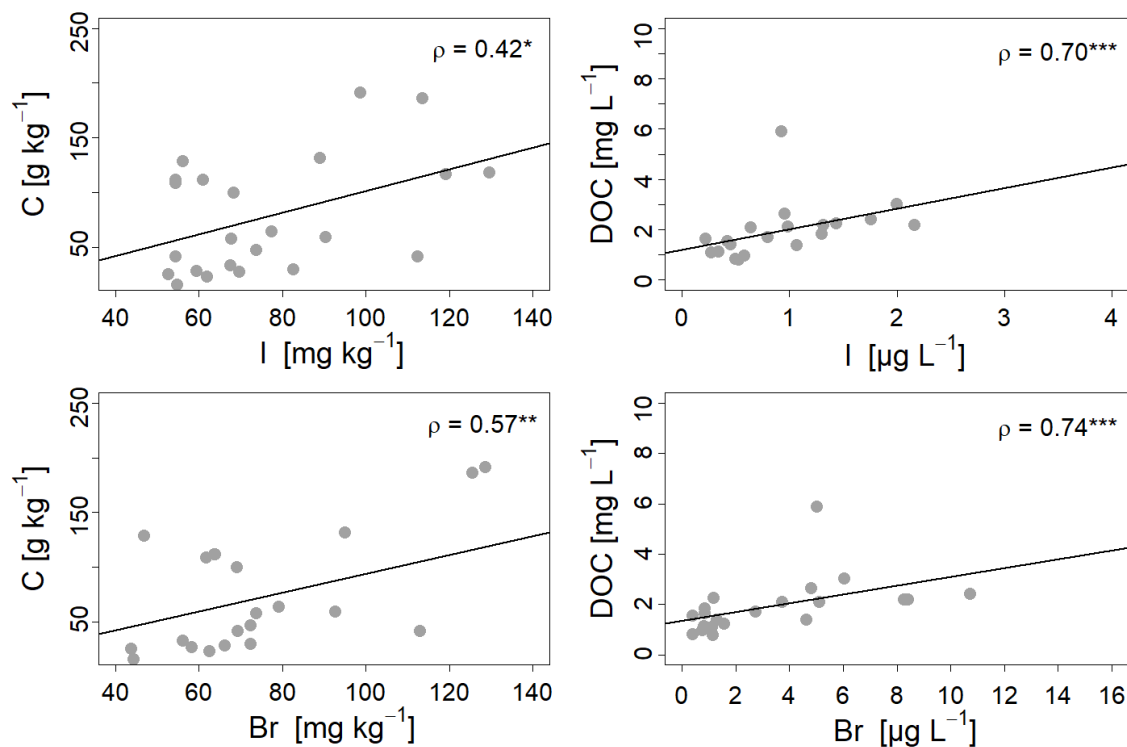


Figure 13: Spearman correlation of *I*-C, *I*-DOC, Br-C and Br-DOC and Spearman correlation coefficient ( $\rho$ ), with \*  $p < 0.05$ , \*\*  $p < 0.01$  and \*\*\*  $p < 0.001$ .

#### 3.3.2 Correlations of I, Br and C with other elements

The spearman correlation coefficient for *I* and Br is  $\rho=0.65$  in leachates and 0.87 in solid samples (Table 8 and Table 7). Rubidium (Rb), chlorine (Cl) and mercury (Hg) showed correlations with Br in solid soil samples ( $0.5 < \rho < 0.7$ ; Table 7). For seven out of 17 elements significant

correlations in solid samples with *I*, Br and C are negative. Strongest correlations occurred between C-N ( $\rho=0.94$ ), C-Si ( $\rho=-0.88$ ) and C-Cl (0.85).

The *I*- and Br values in leachates showed correlations with arsenic (As), yttrium (Y), lanthanum (La), lead (Pb), uranium (U) with a spearman coefficient of  $0.5 < \rho < 0.7$  (Table 8). *I* is correlated with cerium (Ce) and aluminium (Al) ( $\rho \geq 0.7$ ). Br is correlated ( $\rho \geq 0.7$ ) with cerium (Ce), magnesium (Mg) and nitrate ( $\text{NO}_3^-$ ). Correlations in leachates were positive, except for chloride ( $\text{Cl}^-$ ), and strongest for Br- $\text{NO}_3^-$  ( $\rho=0.93$ ), Br-Mg ( $\rho=0.89$ ) and Br-Ca ( $\rho=0.85$ ).

Table 7: Spearman correlation coefficients of *I*, Br and C and all measured elements in solid samples, non-significant correlations are written in grey.

	<i>I</i>	Br	C	N	Mn	Fe	Cl			
<i>I</i>	1	0.87	0.41	0.31	-0.14	-0.31	0.5			
Br	0.87	1	0.58	0.45	-0.03	-0.47	0.61			
C	0.41	0.58	1	0.94	0.16	-0.68	0.85			
								Ni	Cu	As
<i>I</i>	-0.55	-0.28	0.21	0.65	0.13	-0.07	-0.2	0.28	-0.31	0.57
Br	-0.48	-0.3	-0.02	0.7	0.25	0.01	-0.41	0.12	-0.36	0.6
C	-0.22	-0.41	-0.11	0.5	0.45	-0.17	-0.71	0.12	-0.88	0.76

Table 8: Spearman correlation coefficients of *I*, Br and DOC and all measured elements in leachates, non-significant correlations are written in grey.

	<i>I</i>	Br	DOC	Al	Fe	Mg	Mn	Ca		
<i>I</i>	1	0.65	0.7	0.71	0.36	0.61	0.51	0.44		
Br	0.65	1	0.74	0.55	0.08	0.89	0.75	0.85		
DOC	0.7	0.74	1	0.66	0.31	0.69	0.62	0.65		
	As	Y	La	Ce	Pb	U	Cl <sup>-</sup>	NO <sub>3</sub> <sup>-</sup>	SO <sub>4</sub> <sup>2-</sup>	
<i>I</i>	0.54	0.58	0.69	0.77	0.66	0.69	0.3	0.56	0.41	
Br	0.7	0.8	0.69	0.77	0.63	0.6	-0.09	0.93	0.52	
DOC	0.49	0.77	0.75	0.74	0.81	0.66	-0.19	0.7	0.55	

### 3.4 I/Br ratios

Highest ratios in solid samples were found in subsoil horizons ( $\geq 30$  cm) in six out of nine profiles (Figure 14). The maximum was 1.2 (L2 Bw2, 80 cm), the minimum 0.8 (L3 Ah, 5 cm and AhBw, 15 cm) and the median 1.0. The horizons with the lowest I/Br ratios in solid samples of the respective profiles differed among the profiles.

The I/Br ratios in leachates were lower than in solid soil samples, except for four horizons (L2 Bw, L3 Bw, R2 Bw and R4 Ah). The maximum ratio for leachates was 1.6 (R2 Bw, 65 cm), the minimum 0.1 (L4 AhBw, 20 cm) and the median 0.3. In topsoils, leachate I/Br ratios varied with the magnitude of 0.1 around the ratio in the rain water sample (0.3), except for profile R4. The maximum ratios in leachates were found in subsoil horizons ( $\geq 30$  cm) in seven out of nine profiles. Profiles L1, R4 and R5 revealed maximum ratios in leachates from topsoil horizons (5 cm). Horizons containing minimum I/Br ratios in leachates of the respective profiles differed among the profiles.

The median difference between the I/Br ratio of solid samples and leachates was 0.6. The variation of the I/Br ratio was higher in leachates than in solid soil samples where the ratios were close to one. The median variation with depth in solid samples was 0.1, whereas the ratio in leachates showed a mean variation of 0.8 with depth.

Two main patterns could be seen: The first pattern was found in profiles L2, L3, L4, R2 and R3 and showed a similar trend up to 20 cm depth for I/Br ratios in solid samples and leachates. Below 20 cm, ratios of leachates rapidly approached ratios of solid samples. Profile R1 also showed an increase in the leachate I/Br ratio from topsoil to subsoil (difference: 0.5). Ratios in solid samples stayed constant with depth (difference:  $\ll 0.1$ ). But due to the lack of a transitional horizon and the related missing of a third sampling point, the pattern was not as obvious. The second pattern was seen in L1 and R5. It showed only a small change of I/Br ratios with depth in solid samples and in leachates (difference:  $< 0.1$ ). Pattern two seemed to match the top part ( $\leq 20$  cm) of pattern one.

One exception was profile R4. The leachate ratio was lower than in solid samples in topsoil (5 cm), higher than the ratio in solid samples in subsoil (30 cm) and showed a change with depth of 0.9. The ratios in solid samples were rather constant with depth in this profile (change:  $< 0.1$ ).

Even though trends of I and Br concentrations in depth profiles were similar, I/Br ratios revealed that Br seemed to be leached more easily from the soil than I. This difference was particularly noticeable in topsoil and transitional horizons ( $\leq 20$  cm).

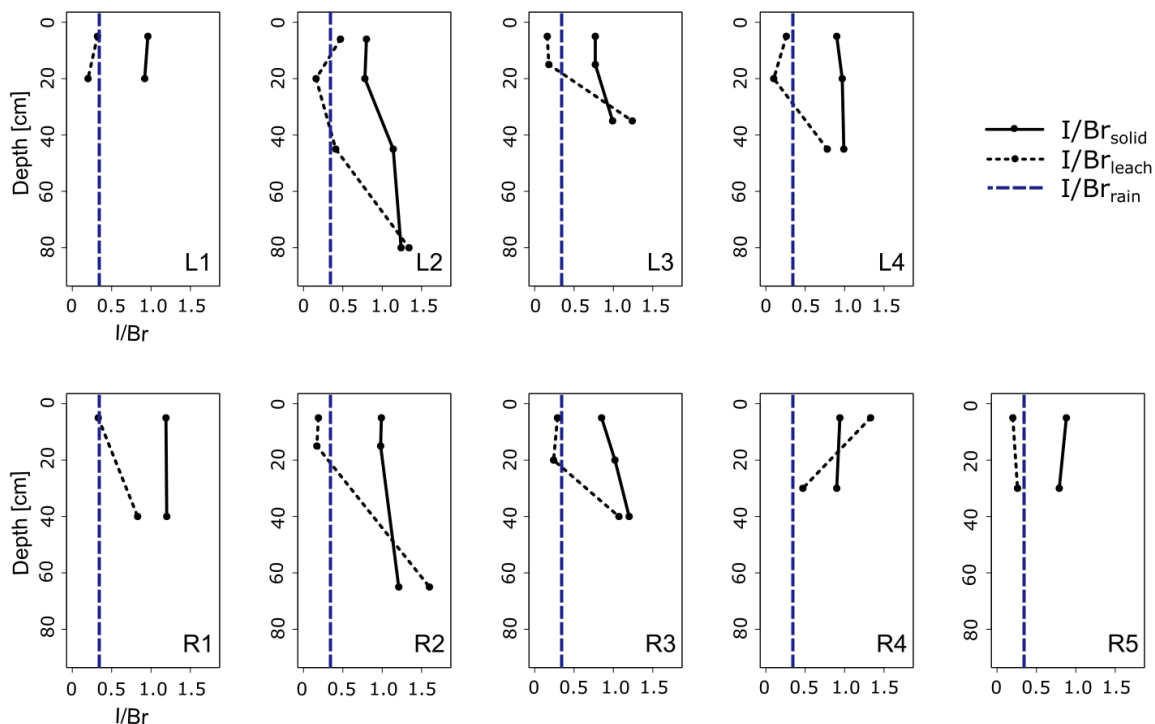


Figure 14: Iodine-bromine-ratios in rain water sample (0.3), solid soil samples and leachates in profiles L1-L4 and R1-R5, shown at the average depth for each sampled horizon (Table 2 and Table 3).

### 3.5 Spatial differences in I, Br, C and Fe concentrations

Figure 15 shows a comparison of medians and variation for solid samples for slope L and slope R. Differences in I, Br, C and Fe in solid samples were most pronounced in topsoils and transitional horizons ( $\leq 20$  cm). Since not all soil profiles showed a transitional horizon, medians are stated for topsoil horizons (5-6 cm). Medians of I, Br and C concentrations were higher on slope L. Differences between the slopes were  $29.9 \text{ mg kg}^{-1}$  for I,  $44.6 \text{ mg kg}^{-1}$  for Br and  $76.9 \text{ g kg}^{-1}$  for C. Fe concentrations were higher on slope R, the difference between the medians was  $25.2 \text{ g kg}^{-1}$ . Values on slope L showed a higher variability, especially in C concentrations. Relative standard deviations in topsoils C concentrations were 46 % on slope L and 12 % on slope R. For I, Br and Fe, relative standard deviations in topsoils were 28 %, 30 % and 40 % on slope L and 23 %, 26 % and 8 % on slope R. However, when interpreting the data, the low number of data points needs to be considered.

In leachates, variations in I, Br, DOC and Fe concentrations among the slopes were high. Standard deviations for Br and Fe were 1.5 and 5 times higher than the median concentrations (Figure 16). For all elements, median concentrations in leachates of slope L were higher than of slope R. The greatest difference between the slopes was in Br concentrations with  $8.8 \mu\text{g L}^{-1}$ . I showed a disparity in medians of  $2.0 \mu\text{g L}^{-1}$ . Differences in median DOC and Fe concentrations were  $2.2 \text{ mg L}^{-1}$  and  $2.8 \mu\text{g L}^{-1}$  respectively.

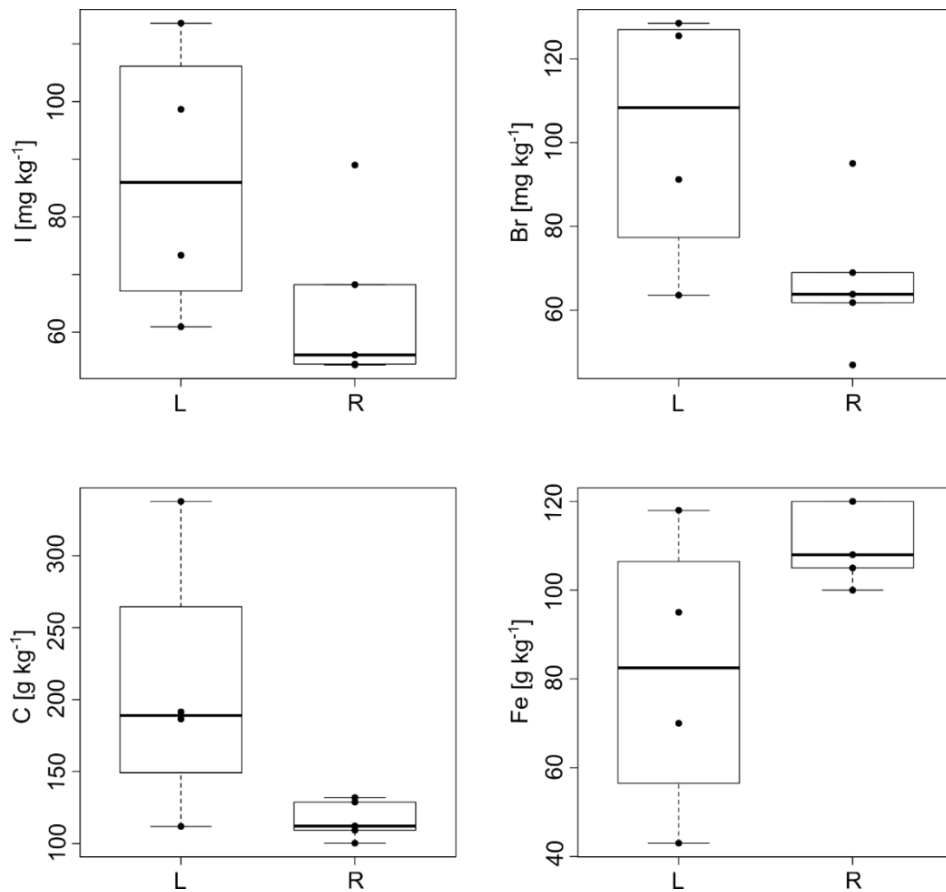


Figure 15: Boxplot of iodine (I) [ $\text{mg kg}^{-1}$ ], bromine (Br) [ $\text{mg kg}^{-1}$ ], carbon (C) [ $\text{g kg}^{-1}$ ] and iron (Fe) [ $\text{g kg}^{-1}$ ] concentrations in solid samples of topsoil horizons (5-6 cm) on slope L and R, shown at the average depth for each sampled horizon (Table 2 and Table 3), black lines show medians, black dots represent data points, boxes cover the 25 % and 75 % quartile, whiskers extend to 1.5-fold extension of the respective box.

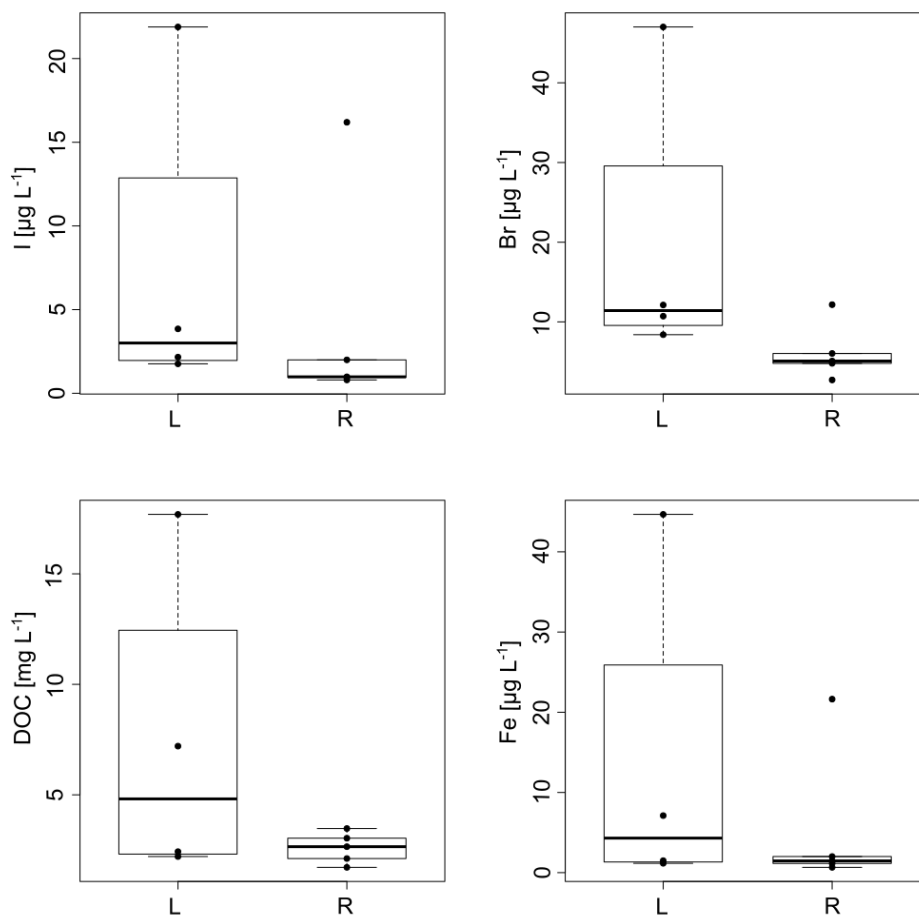


Figure 16: Boxplot of iodine (I) [ $\mu\text{g L}^{-1}$ ], bromine (Br) [ $\mu\text{g L}^{-1}$ ], dissolved organic carbon (DOC) [ $\text{mg L}^{-1}$ ] and iron (Fe) [ $\mu\text{g L}^{-1}$ ] concentrations in solid samples of topsoil horizons (5-6 cm) on slope L and R, shown at the average depth for each sampled horizon (Table 2 and Table 3), black lines show medians, black dots represent data points, boxes cover the 25 % and 75 % quartile, whiskers extend to 1.5-fold extension of the respective box.

### 3.6 Accumulation vs. depletion of nutrients

The data shows that N, potassium (K), manganese (Mn) and zinc (Zn) were depleted in the solid soil of the ReBAMB (Table 9). But the soils were enriched in copper (Cu) and Fe. Calcium (Ca) concentrations were in the range of typical values from temperate zones.

The measured element concentrations in leachates represent water soluble nutrient contents, available for plant uptake. Concentrations of Fe,  $\text{NO}_3^-$  and  $\text{SO}_4^{2-}$  in leachates were clearly lower than typical values reported for soil solutions in temperate zones (Table 10; Blum, 2012). Values for phosphate, nitrite, bromide and fluoride were below detection limits. This underlines the nutrient deficiency of the soils in the ReBAMB.

Detailed nutrient concentrations in solid samples and leachates are listed in Appendix 6 and Appendix 7.

Table 9: Typical values and mean of main- and trace nutrient concentrations in solid soil samples, high mean concentrations in relation to typical values are printed in italic, low mean concentrations in bold.

Soil profile	<i>Fe</i> [g kg <sup>-1</sup> ]	<i>N</i> [g kg <sup>-1</sup> ]	<i>K</i> [g kg <sup>-1</sup> ]	<i>Ca</i> [g kg <sup>-1</sup> ]	<i>Mn</i> [g kg <sup>-1</sup> ]	<i>Cu</i> [mg kg <sup>-1</sup> ]	<i>Zn</i> [mg kg <sup>-1</sup> ]
Typical values*	5-40	3-30	2-30	2-15	0.2-4	5-100	10-300
Mean	<i>112</i>	<b>8.1</b>	<b>2</b>	8	<b>1.1</b>	<i>111</i>	<b>81</b>
Min	42.7	2.4	1	5	0.3	41.0	55.8
Max	175.8	20.3	2	15	2.0	205.0	129.7

\* Blum (2012)

Table 10: Typical values, mean and median Iron (Fe) [ $\mu\text{g L}^{-1}$ ], Chloride (Cl<sup>-</sup>) [mg L<sup>-1</sup>], Nitrate (NO<sub>3</sub><sup>-</sup>) [mg L<sup>-1</sup>] and Sulfate (SO<sub>4</sub><sup>2-</sup>) [mg L<sup>-1</sup>] concentrations in leachates. Low mean concentrations in relation to typical values are marked in bold.

	<i>Fe</i> [ $\mu\text{g L}^{-1}$ ]	<i>Cl<sup>-</sup></i> [mg L <sup>-1</sup> ]	<i>NO<sub>3</sub><sup>-</sup></i> [mg L <sup>-1</sup> ]	<i>SO<sub>4</sub><sup>2-</sup></i> [mg L <sup>-1</sup> ]
Typical values*	< 100	-	10-200	10-200
Mean	<b>6.5</b>	0.9	<b>7.7</b>	<b>1.5</b>
Median	<b>1.5</b>	0.8	<b>4.2</b>	<b>1.5</b>
Min	0.1	0.5	0.2	0.5
Max	44.7	1.6	23.7	3.3

\* Blum (2012)

### 3.7 Pore water samples – Depth profiles of element concentrations

Element concentrations in pore water samples were variable and did not show any specific patterns (Table 11). *I* concentrations decreased with depth in profiles L2 and R2 and increased with depth in L1. The maximum *I* concentration was 3.6  $\mu\text{g L}^{-1}$  and was measured in the pore water of the topsoil horizon in profile R2 (5 cm). Br also showed decreasing concentrations with depth and a maximum concentration of 35.2  $\mu\text{g L}^{-1}$  in the topsoil horizon of profile L2 (6 cm).

DOC and nitrate (NO<sub>3</sub><sup>-</sup>) depth trends could not be detected because for both elements two out of seven samples did not provide enough fluid to conduct the measurement. The maximum DOC concentration in the pore water samples was 11.0 mg L<sup>-1</sup> (L2 AhBw, 20 cm) and the minimum 1.6 mg L<sup>-1</sup> (R2 AhBw, 15 cm). For NO<sub>3</sub><sup>-</sup>, the minimum was 0.1 mg L<sup>-1</sup> (R2 Ah, 5 cm) and the maximum 3.2 mg L<sup>-1</sup> (L1 Ah, 5 cm). Fe values showed high variation with a maximum of 35.3  $\mu\text{g L}^{-1}$  (R2 Ah, 5 cm) and a minimum of 1.5  $\mu\text{g L}^{-1}$  (R2 AhBw, 15 cm). Chloride (Cl<sup>-</sup>) and sulfate (SO<sub>4</sub><sup>2-</sup>) concentrations decreased with depth, except for Profile L2 where SO<sub>4</sub><sup>2-</sup> increased slightly from transitional (20 cm) to subsoil horizon (45 cm).

Table 11: Dissolved organic carbon (DOC) [ $\text{mg L}^{-1}$ ], Iodine (I) [ $\mu\text{g L}^{-1}$ ], Bromine (Br) [ $\mu\text{g L}^{-1}$ ], Iron (Fe) [ $\mu\text{g L}^{-1}$ ], Chloride (Cl) [ $\text{mg L}^{-1}$ ], Nitrate ( $\text{NO}_3^-$ ) [ $\text{mg L}^{-1}$ ] and Sulfate ( $\text{SO}_4^{2-}$ ) [ $\text{mg L}^{-1}$ ] in pore water samples.

Soil profile	DOC [ $\text{mg L}^{-1}$ ]	I [ $\mu\text{g L}^{-1}$ ]	Br [ $\mu\text{g L}^{-1}$ ]	Fe [ $\mu\text{g L}^{-1}$ ]	Cl <sup>-</sup> [ $\text{mg L}^{-1}$ ]	NO <sub>3</sub> <sup>-</sup> [ $\text{mg L}^{-1}$ ]	SO <sub>4</sub> <sup>2-</sup> [ $\text{mg L}^{-1}$ ]
L1 Ah (5 cm)	2.8	0.6	4.7	7.7	3.5	3.2	1.4
L1 II AhBw (20 cm)	4.2	1.0	2.7	15.9	1.7	0.2	0.8
L2 Ah (6 cm)	NA	2.4	35.2	12.4	NA	NA	NA
L2 AhBw (20 cm)	11.0	1.7	23.9	20.5	4.1	0.3	0.5
L2 Bw1 (45 cm)	2.9	0.6	18.5	0.7	3.9	NA	0.6
R2 Ah (5 cm)	NA	3.6	25.0	35.3	5.0	0.1	0.9
R2 AhBw (15 cm)	1.6	0.3	5.8	1.5	3.1	NA	0.6

NA = data not available

## 4 Discussion

### 4.1 *I* and Br status in the soils of the ReBAMB

#### 4.1.1 High *I* and Br contents in solid soil samples and low leachability

The measured *I* concentrations in solid samples were high compared to those reported from previous studies. The maximum was 130 mg kg<sup>-1</sup> (L2 AhBw, 20 cm) and the median 69 mg kg<sup>-1</sup> (Figure 8). Typical *I* concentrations for soils worldwide range from <0.1 to 10 mg kg<sup>-1</sup>, up to 100 mg kg<sup>-1</sup> in volcanic ash soils (Kabata-Pendias, 2011) and up to 660 mg kg<sup>-1</sup> in highly organic soils in close proximity to the ocean (Smyth and Johnson, 2011).

Br concentrations in the investigated soils were also elevated compared to other studies. The maximum Br concentration in solid samples was 165 mg kg<sup>-1</sup> (L2 AhBw, 20 cm) and the median 71 mg kg<sup>-1</sup> (Figure 8). An average Br content in soils of 10 mg kg<sup>-1</sup> is stated in the literature, the lowest values were found in podzols (Kabata-Pendias, 2011). For volcanic ash soils values above 100 mg kg<sup>-1</sup> can be reached (Kabata-Pendias, 2011). High organic matter content and long exposure time can lead to Br concentrations in soils up to 299 mg kg<sup>-1</sup> (Martínez Cortizas et al., 2016).

In contrast to high *I* and Br contents in solid samples, only a small proportion was leachable (*I*: median 0.9 µg L<sup>-1</sup>, Br: median 3.2 µg L<sup>-1</sup>; Figure 11). The median water leachable fractions from soils in the ReBAMB were 0.01 % for *I* and 0.04 % for Br (Figure 12). This stands in line with the findings of Martínez Cortizas et al. (2016) where all Br in the soil was non-water soluble. However, water leachable *I* and Br fractions up to 10 % were reported from Johnson (1980).

The high concentrations in solid soil and small leachable fractions suggest a high retention capacity in the soils of the ReBAMB, leading to *I* and Br accumulation.

#### 4.1.2 *I* and Br accumulation in soils

Continuous *I* and Br input occurs through precipitation. In topsoils, *I* and Br are fixed with OM. Small amounts of *I* and Br can be remobilised and gradually transported downwards in association with DOC. With increasing abundance of Fe-Oxides in transitional horizons (15-20 cm) and subsoils (≥30 cm), the *I*-DOC and Br-DOC complexes are immobilised. This inhibits further *I* and Br leaching. These processes reveal the importance of OM for *I* and Br fixation and mobilisation. The significance of Fe-Oxides for *I* and Br immobilisation is higher in the soils of the ReBAMB than in soils of temperate zones, due to high Fe contents (median: 114 g kg<sup>-1</sup>). The immobility of Fe is highlighted by low Fe concentrations in leachates and pore water samples (Figure 10, Table 10 and Table 11). Consequently, constant *I* and Br input since soil

formation  $9 \times 10^6$  years ago and the high fixation potential of the soils in the ReBAMB result in *I* and Br accumulation.

## 4.2 Processes determining *I* and Br accumulation in the soils of the ReBAMB

### 4.2.1 *I* and Br sources to soils

The *I* and Br content in soils is controlled by the *I* and Br supply and the retention capacity of the soils. The latter appears to be high in the investigated soils. (1) Precipitation and (2) bedrock material are the two possible *I* and Br sources in the study area.

#### Precipitation is the main *I* and Br source

*I*/Br ratios in leachates of topsoils (5-6 cm) and transitional soil horizons (15-20 cm), varied by only 0.1 around the ratio in canopy throughfall water (Figure 14). This leads to the assumption that precipitation is the main *I* and Br source for the soils in the ReBAMB. The analysis of a throughfall sample in the study area showed an *I* concentration of  $1.42 \mu\text{g L}^{-1}$  and a Br concentration of  $5.0 \mu\text{g L}^{-1}$  (Piechulla, 2018). Since canopy throughfall was sampled, it includes the *I* and Br washed off from leaves and lacks interception. Therefore, it shows the approximate chemical composition of the rainfall that reaches the soil. The measured *I* concentration in canopy throughfall was slightly lower than the range of rainwater ( $1.5\text{-}2.5 \mu\text{g L}^{-1}$ ) given by Whitehead (1984) for temperate zones. Combining these values with the high annual rainfall in the ReBAMB ( $3.6 \text{ m a}^{-1}$ ), leads to annual *I* and Br depositions of  $5.1 \text{ mg m}^{-2}$  and  $18 \text{ mg m}^{-2}$ , respectively. A high percentage of the *I* input from wet deposition is likely to enter the soil despite vegetation cover (Whitehead, 1984). This implies a deposition of  $4.6 \times 10^7 \text{ mg m}^{-2}$  *I* and  $16.2 \times 10^7 \text{ mg m}^{-2}$  Br on the soils of the ReBAMB since the beginning of soil formation  $9 \times 10^6$  years ago.

Also previous studies came to the conclusion that atmospheric input is the main natural *I* and Br source for soils (Fuge and Johnson, 1986; Låg and Steinnes, 1976; Smyth and Johnson, 2011; Whitehead, 1984; Yuita and Kihou, 2005).

Plants take up *I* from the atmosphere through stomata. The uptake increases with increasing humidity (Barry and Chamberlain, 1964). Due to constantly humid conditions in ReBAMB (annual average relative humidity: 98 %), plant uptake of *I* is probably high, compared to temperate regions. In undisturbed ecosystems, the *I* that is contained in vegetation is returned to the soil through the decomposition of dead plant material (Fuge and Johnson, 1986; Whitehead, 1984).

### **Low contribution from bedrock**

High *I* concentrations and intensive weathering conditions in the investigated soils suggest a high release of *I* from bedrock to the soils. But analyses of bedrock samples, in the study area, showed that *I* contents are below 1 mg kg<sup>-1</sup> and Br contents below 2 mg kg<sup>-1</sup> (Piechulla, 2018). This indicates a low contribution of *I* and Br input from bedrock to the soils in the ReBAMB. Fuge and Johnson (1986) reviewed on the *I* input from bedrock material to soils and concluded that despite the fact that *I* is enriched during the weathering process, its contribution is low. This is supported by other studies: Smyth and Johnson (2011) found no relationship between soil *I* content and bedrock lithology. Yuita and Kihou (2005) suppose that the *I* contribution from parent material in Andosols is low enough to be disregarded. Only for soils on marine sediment, *I* and Br contributions from bedrock might be more relevant, due to elevated concentrations in marine environments (Whitehead, 1984; Wisniak, 2002). Volcanic emissions can contribute considerably to Br, but only to a lesser extent to *I* input (Aiuppa et al., 2005). This can also be seen from estimated global *I* and Br fluxes, which are 0.11 kt yr<sup>-1</sup> and 13 kt yr<sup>-1</sup> respectively (Aiuppa et al., 2005).

Along with these findings, bedrock can be considered to only deliver a minor *I*- and Br input fraction to the soils of the ReBAMB. Whereas volcanic ashes might have contributed to the Br but not to the *I* content of the investigated soils.

#### **4.2.2 Sorption of *I* and Br to OM**

After *I* and Br entered the soil through precipitation, sorption to OM resulted in rapid immobilisation. This is supported by maximum *I* and Br concentrations in depths  $\leq 20$  cm in solid soil samples from six (*I*) and seven (Br) out of nine profiles (Figure 8). Particularly the topsoil and the transitional horizon of profile L2, where the highest C concentrations were found, reveal the highest *I* and Br concentrations among the profiles. The correlation of *I* and Br with C in solid samples was weak (*I*-C: 0.42, Br-C: 0.57; Figure 13), but previous research has shown that *I* and Br have a high affinity for OM and are readily and strongly bound to it (Biester et al., 2004; Leri and Myneni, 2012; Martínez Cortizas et al., 2016; Smyth and Johnson, 2011; Xu et al., 2011a). A reason for the weak correlation between *I* and Br with C in solid samples might be the high carbon content (median: 62 g kg<sup>-1</sup>). This results in the fact that C is not a limiting factor for *I*- and Br fixation. Hence, increasing C concentrations do not lead to a stronger selective *I*- and Br fixation.

*I* is oxidised and bound to OM more easily than Br, due to its lower electronegativity. Natural Br oxidation and therefore bromination of OM is dependent on the activity of haloperoxidases

(Wever and van der Horst, 2013). To a smaller extent, abiotic bromination of OM in the presence of hydrogen peroxide or ferric iron is also possible (Leri and Ravel, 2015). Hence, *I* and Br are fixed by OM in topsoils and transitional soil horizons, lowering Br- but especially *I* mobility. This verifies hypothesis 1.

A modelling study on radioiodine biogeochemistry demonstrated the time dependence of *I* sorption (Chang et al., 2014). In the first two weeks *I* was shown to be reversibly bound to SOM. From that point on, an irreversible binding of *I* to SOM took place (Chang et al., 2014). This is confirmed by the batch experiments from Shetaya et al. (2012), who found a slower sorption of  $\text{IO}_3^-$  in the presence of OM. This matches the theory of *I* mobilisation in topsoils shortly after incorporation into the soil.

#### **4.2.3 Association of other elements with OM**

C shows positive correlations with N ( $\rho=0.94$ ), Cl ( $\rho=0.85$ ) and Hg ( $\rho=0.76$ ; Table 7) in solid soil. All of these elements occur mainly in organically bound form in soils (Renneberg and Dudas, 2001; Scheffer et al., 2010; Yuita, 1983). Negative correlations of C with Zr ( $\rho=-0.71$ ), Si ( $\rho=-0.88$ ) and Fe ( $\rho=-0.68$ ) might be attributed to a dilution effect. Zr, Si and Fe originate from minerals. With rising OM content in topsoils, the percentage of the mineral phase is reduced.

#### **4.2.4 Mobilisation of *I* and Br through DOC**

Forms of *I* in soil solutions are SOI,  $\text{IO}_3^-$  and *I*, whereas SOI comprises more than half of the total soluble *I* (Xu et al., 2011b). *I* can also be transported in form of COI in association with colloidal organic matter (Xu et al., 2011b; Xu et al., 2011a).

Positive correlations reveal a DOC-associated transport of *I* and Br (*I*-DOC: 0.7, Br-DOC: 0.74; Figure 13). This is supported by maximum leachable *I*- and Br fractions (*I*: 0.4 %, Br: 0.6 %) in topsoil horizons (5-6 cm; Figure 12), where maximum DOC concentrations were found (Figure 9). *I*-DOC and Br-DOC complexes are transported to transitional- (15-20 cm) and subsoil horizons ( $\geq 30$  cm). Previous studies stated that 54-56 % (Xu et al., 2011b) and 83 % (Yamada et al., 1999) of mobile *I* is bound to humic- and fulvic acids in organic rich soils. Therefore, DOC is thought to determine the *I* transport in soils (Santschi et al., 2017; Whitehead, 1984).

The crucial role of DOC for *I*- and Br transport is further highlighted by the comparison of the results from the soils in the ReBAMB with the studies of Kuss (2018). The study investigated *I*- and Br contents, speciation and mobility in a Podzol and a Rendzic Leptosol in Lower Saxony, Germany. Maximum *I*- and Br concentrations in solid soil samples of the two profiles (*I*: 11 mg kg<sup>-1</sup>, Br: 15 mg kg<sup>-1</sup>) comprised only 16 % (*I*) and 21 % (Br) of the median *I* and Br

values in the ReBAMB (*I*: 69 mg kg<sup>-1</sup>, Br: 71 mg kg<sup>-1</sup>). But water leachable *I* fractions made up 8 % on average in the Podzol profiles and 5 % in the Rendzic Leptosol. For Br, water leachable fractions accounted for 17 % and 11 % in the Podzol and Rendzic Leptosol respectively. The high mobility of *I* and Br stands in contrast with our findings, where median leachable *I*- and Br fractions were 0.01 % and 0.04 % respectively. Thus, water leachable fractions were higher compared to the soils of the ReBAMB, despite lower total *I*- and Br contents in solid samples. The DOC concentrations in the Podzol (mean: 122 mg L<sup>-1</sup>) and the Rendzic Leptosol (mean: 88 mg L<sup>-1</sup>) clearly exceed the DOC concentrations in the soils in the ReBAMB (median: 2 mg L<sup>-1</sup>). This results in a higher *I*- and Br mobilisation potential. Also, Fe concentrations in solid samples are lower (mean Podzol: 1.1 g kg<sup>-1</sup>, mean Rendzina: 28.7 g kg<sup>-1</sup>) than in this study (median: 114 g kg<sup>-1</sup>), leading to a lower *I* and Br retention capacity.

#### **4.2.5 Mobilisation of other elements through DOC**

DOC shows a correlation with all measured elements with a spearman correlation coefficient of  $\rho > 0.6$ , except for As ( $\rho = 0.49$ ) and SO<sub>4</sub><sup>2-</sup> ( $\rho = 0.55$ ; Table 8). This results in an indirect correlation of *I* and Br with these elements, due to the correlation between *I*, Br and DOC. The correlations of DOC, *I* and Br with Al, As and Pb might be attributed to DOC associated transport, as these three elements are known for a high affinity to OM (Bauer and Blodau, 2006; Jansen et al., 2005; Sauvé et al., 1998). All correlations in leachates, except for Br-Cl and DOC-Cl, are positive. This may be attributed to the experimental setup. In batch leaching experiments, all elements are washed out intensively due to the long shaking time.

#### **4.2.6 Low DOC concentrations due to DOC stabilisation and decomposition**

The DOC concentration in leachates (median 2.0 mg L<sup>-1</sup>) and pore waters (median 2.9 mg L<sup>-1</sup>) was low (Figure 9 and Table 11), even though the C contents of the upper soil horizons were high (median: 62 g kg<sup>-1</sup>; Figure 9). On slope L, higher inclination lead to less rainwater infiltration into soils, more surface runoff and therefore less DOC mobilisation than on slope R. This resulted in higher leachate DOC concentrations on slope L (median DOC slope L: 2.2 mg L<sup>-1</sup>, slope R: 1.8 mg L<sup>-1</sup>; Figure 16). In pore waters from temperate zones, DOC concentrations between 18 mg L<sup>-1</sup> and 29 mg L<sup>-1</sup> were found (Troyer et al., 2011; van den Berg et al., 2012). DOC concentrations in a stream discharging from a peat bog in Germany most closely approximate the DOC concentrations in this study with 5-30 mg L<sup>-1</sup> (Broder and Biester, 2015). But these are still higher than the DOC concentrations in leachates from the soils of the ReBAMB, even if DOC is highly diluted in stream waters.

Low DOC concentrations in soil solutions were previously observed in Andosols and tropical soils (Aran et al., 2001; Camino-Serrano et al., 2014). This was explained by the stabilisation

of SOM through the sorption to amorphous minerals and the formation of highly stable organo-metallic complexes. Also the soils in the ReBAMB exhibited high Fe contents (median Fe: 114 g kg<sup>-1</sup>) compared to soils in temperate zones. This promotes effective SOM and DOC stabilisation, increasing with soil depth (Hagedorn et al., 2015; Kaiser et al., 1996). Organo-metallic complexes are protected against disaggregation by water and microbial degradation. Therefore, a major fraction of SOM is not available for decomposition, resulting in a lower DOC release (Aran et al., 2001; Camino-Serrano et al., 2014). The stabilisation of C originating from root residues is further promoted in topsoils of the ReBAMB due to high root abundance and therefore high root-soil-interaction (Oades, 1988). The same process is conceivable for DOC originating from root exudates. In solutions of tropical soils, DOC concentrations are reported to be low due to preferential moisture- and air temperature conditions. This results in the promotion of microbial decomposition of unbound DOM (Aran et al., 2001; Camino-Serrano et al., 2014; Cleveland et al., 2004).

Contrary to the low DOC concentrations in the soils of the ReBAMB, elevated DOC values were expected due to accumulation during the dry season. The reason for the latter is the lower washout during the dry season due to less precipitation and the lower groundwater level (Humbert et al., 2015). This indicates, that DOC is degraded or stabilised in the soil rapidly after formation.

The most salient difference between the soils in the ReBAMB and soils in temperate zones is the high Fe content (median Fe: 114 g kg<sup>-1</sup>). This promotes effective DOC stabilisation, increasing with soil depth (Hagedorn et al., 2015; Kaiser et al., 1996). This falsifies hypothesis 3, because DOC concentrations are not only low due to degradation but also due to stabilisation by Fe-Oxides.

As the main determinant for *I*- and Br mobility, low DOC concentrations are the limiting factor for *I* and Br leaching from the soils in the ReBAMB.

#### **4.2.7 Stabilisation of dissolved organic *I*- and Br complexes by Fe-Oxides**

If *I*-DOC and Br-DOC complexes are not re-adsorbed by SOM in topsoils, a transport to deeper soil horizons is possible. Fe contents rose clearly beneath topsoil horizons (Figure 10). Thus, transitional- (15-20 cm) and subsoil horizons (≥30 cm) provide a high fixation potential for *I*-DOC and Br-DOC complexes. *I* concentrations in leachates of transitional- (15-20 cm) and subsoil horizons (≥30 cm) were close to zero with a leachable fraction of 0.01 %, which indicates almost no mobility and strong fixation (Figure 11). Br particularly showed a small leachable fraction in subsoil horizons (≥30 cm; mean: 0.02 %). Thus, *I* and Br were retained here.

Likely only small amounts reached the subsoil ( $\geq 30$  cm) due to retention in transitional soil horizons (15-20 cm).

In profile L4, the rise in Fe content was small from topsoil (5 cm) to the transitional horizon (20 cm), but great from the transitional- to the subsoil horizon (45 cm) (Figure 10). Therefore, mobile *I* and Br passed the transitional horizon and were fixed in the subsoil. This was seen from maximum *I* concentrations in profile L4 in the subsoil (Figure 8) and highlights the role of Fe-Oxides for *I* retention. For profile R4, a similar pattern is likely. A horizon with elevated Fe, *I* and Br concentrations might be found in greater depths.

A long-term fixation of *I* and Br seems to happen through Fe-Oxides in transitional horizons (15-20 cm) and subsoils ( $\geq 30$  cm). Whereas C in topsoils (5-6 cm) and transitional horizons (15-20 cm) seems to play a role for both, long-term fixation and short-term fixation with subsequent DOC-associated transport. Results from a solid phase sequential extraction showed that metal oxides are the main *I* retention factor in the soils of the ReBAMB (Piechulla, 2018). The median of metal oxide associated *I* was 79 % with the highest percentages in transitional horizons (15-20 cm) and subsoils ( $\geq 30$  cm; Piechulla, 2018). High positive relationships and sorption of *I* to Fe- and Al-oxides was also reported in other studies (Whitehead, 1978; Yoshida et al., 1992). The relationship is further increasing with decreasing pH (Whitehead, 1973). Thus, sorption of *I*-DOC complexes by Fe-Oxides result in a prevention of *I* transport, particularly in transitional horizons and subsoils. This verifies hypothesis 2.

Similar to the correlation of *I* and Br with C in solid samples, the generally high soil Fe content (median  $114 \text{ g kg}^{-1}$ ) may obscure the correlation of *I* and Br with Fe (Table 7). Another factor that might weaken the correlations of *I* and Br with C and Fe, despite existing interactions, are differing fixation processes in top- and subsoil. In topsoil, C was more abundant than Fe and therefore likely plays a greater role in *I* and Br fixation. The C content decreased with increasing depth, but the abundance of Fe-Oxides rose (Figure 9 and Figure 10). Thus, Fe-Oxides control the *I* and Br fixation in subsoil. This results in an offset of correlations between C and Fe with *I* and Br.

#### **4.2.8 The role of soil texture, bulk density and air temperature for *I* and Br fixation**

Soil texture became finer with depth in all profiles (Table 2 and Table 3). This might contribute to higher *I*- and Br fixation (Dissanayake et al., 2007; Martínez Cortizas et al., 2016) due to the increased surface available for sorption. Along with the finer texture and the lower content of SOM, the bulk density increased and therefore the permeability of the soils decreased. This further enhances the retention of mobile *I*- and Br forms. Also, the mean annual air temperature of  $21 \text{ }^{\circ}\text{C}$  and the low pH in the ReBAMB supports *I* fixation (Shetaya et al., 2012).

In conclusion, the combination of high SOM and Fe-Oxide contents, finer soil texture and higher bulk density in transitional horizons (15-20 cm) compared to topsoil horizons (5-6 cm), provides preferential conditions for *I* and Br retention.

#### **4.2.9 *I* and Br volatilisation and plant uptake**

*I* and Br can be volatilised from soils in form of CH<sub>3</sub>I and CH<sub>3</sub>Br. For acidic soils and soils with high microbial activity, abiotic and biotic formation of volatile CH<sub>3</sub>I was reported (Allard and Gallard, 2013). Terrestrial CH<sub>3</sub>Br release was suggested for tropical soils by Wever and van der Horst (2013). But high C contents in upper soil horizons (median topsoil: 128.8 g kg<sup>-1</sup>) in the investigated soils of the ReBAMB probably inhibit *I* volatilisation through strong fixation (Whitehead, 1981).

Another pathway for *I* loss from soils is plant uptake via roots. The low bioavailability of *I* in soils with a high *I* fixation potential, like the soils in the ReBAMB, makes this proportion small (Dissanayake et al., 2007). *I* is taken up by plants primarily from the atmosphere through stomata (Whitehead, 1984). For Br, root-uptake might be higher as soil is the main Br source for plants (Shtangeeva, 2017). But Br uptake through plant leaves is also possible (Paradellis and Panayotakis, 1980). However, *I* and Br are returned to the soil during the decomposition of plant residues. Therefore, this pathway is not regarded to considerably contribute to the *I*- and Br loss from the soils in the ReBAMB.

#### **4.2.10 Role of soil erosion for *I* and Br distribution**

Erosion and accumulation processes in the tropics are widespread due to regular heavy rainfall. This results in the interruption of pedogenic processes and the translocation of vast amounts of soil. While eroded soils are shallow and show a partly or complete lack of topsoil horizons, accumulation sites show thick topsoil horizons or possibly buried fossil topsoil horizons. Therefore, erosion and accumulation processes can significantly influence the element distribution on slopes.

The occurrence of erosion events on slope L is evidenced by the finding of Colluvic Cambisols that made up three out of four soil profiles (L1, L3, L4; Table 2). These show that erosion took place despite dense vegetation cover and high infiltration capacities of the soils. This can be attributed to the higher maximum inclination and the rough land surface on slope L. Since the extremely steep parts of the slope could not be accessed, samples were only taken at less steeper sites, where accumulation of eroded material takes place. This could explain higher C-, *I*- and Br contents on slope L than on slope R and most pronounced differences in topsoils and transitional soil horizons. The same process is conceivable for silt and clay particles, which also

showed a higher percentage in profiles on slope L than on slope R (Table 2 and Table 3). Erosion and accumulation processes probably also account for the higher variability in *I*, Br, C and Fe concentrations in solid samples and leachates (Figure 15 and Figure 16).

The absence of colluvic soils on slope R (Table 3) demonstrate that only small or no erosion events occur on this side of the study area. This corresponds with the smaller maximum inclination and the more even land surface. Also, the depth profiles show a more even pattern on slope R and differences between the profiles are clearly smaller than on slope L (Figure 8, Figure 9, Figure 10, Figure 11). Fe contents give further support, these were higher on slope R (median: 120 g kg<sup>-1</sup>) than on slope L (median: 102 g kg<sup>-1</sup>; Figure 10). The lack of erosion events enables undisturbed and therefore stronger weathering of the soils which releases Fe-Oxides.

#### **4.2.11 *I*- and Br accumulation vs. nutrient depletion**

Not only *I*, Br and DOC, but also major ion concentrations (Cl<sup>-</sup>, SO<sub>4</sub><sup>2-</sup> and NO<sub>3</sub><sup>-</sup>) were low in leachates (Table 10). This suggests the depletion of leachable nutrients in the investigated soils. High rainfall and the age of the study area result in extensive and continuous leaching, which is typical for tropical areas (Dissanayake et al., 2007).

In solid soil, *I*, Br, Fe and Cu were enriched, while N, K, Mn and Zn were depleted (Figure 8 and Table 9). Fe was released and relatively accumulated during bedrock weathering. The mean Fe concentration in bedrock samples was 79 g kg<sup>-1</sup> (Piechulla, 2018). K, Mn, Cu and Zn also originate from bedrock weathering and are involved in nutrient cycles between soils and plants. Mean K, Mn, Cu and Zn concentrations in bedrock samples were much smaller than for Fe and ranged between 0.1 g kg<sup>-1</sup> and 2.4 g kg<sup>-1</sup> (Piechulla, 2018). The leachable amounts were higher for K, Mn and Zn than for Fe and Cu. Combined with low replenishment from weathering, this lead to a depletion of these elements, while Fe and Cu were enriched. Despite *I* and Br were leached in greater amounts than the other elements, *I*- and Br accumulation took place due to constant input from the atmosphere.

#### **4.2.12 Comparison of pore water samples and leachates**

Element concentrations in pore water samples and leachates showed distinct differences (Table 10, Table 11, Figure 9, Figure 10 and Figure 11). The high variability of soil-water ratios in the field and the punctual extraction of pore water, makes a direct comparison of pore water samples and leachates challenging. Concentrations of *I*, Br, DOC, Fe and ions in pore waters resulted in extreme spatial variations. Leachates provided more representative values of the water-soluble fractions, since they included mixed samples from each soil horizon. The low soil-water ratio and the long shaking time increased physical disturbance of aggregates and therefore increased the available surface area for the leaching of elements. Therefore, leachates give

an estimation of theoretically leachable element fractions and concentration trends in depth and space, while pore water samples give an idea of “natural” element concentrations in the soil solution.

### 4.3 Comparison of *I* and Br soil chemistry

#### 4.3.1 Differences in *I* and Br soil chemistry – Correlations and *I*/Br ratios

The Spearman correlation coefficients show a similarity between *I* and Br soil chemistry. This correlation is stronger in solid soil samples ( $\rho = 0.87$ ; Table 7) than in leachates ( $\rho = 0.65$ ; Table 8). The comparison between *I*/Br ratios in leachates and solid samples with the ratio in rain water, allows conclusions about differences in *I* and Br soil chemistry. The *I*/Br ratio of 0.3 in a rain water sample (calculated with values from Piechulla, 2018) was set as the reference point for comparisons of *I*/Br ratios in leachates as it represents the initial concentration ratio of *I* and Br input to the soil.

The ratios in eight out of thirteen leachates from topsoils and transitional horizons, showed lower values than in rain water (mean difference: 0.1; Figure 14). This indicates a higher mobility of Br in relation to *I* and is supported by *I*/Br ratios close to one in solid samples. The latter indicate similar *I* and Br concentrations in solid soil, despite a more than 3.5 times higher input of Br than *I*. As a result, *I* retention is stronger than Br retention. Therefore, Br is washed out to the river or is taken up by plants, whereas *I* is fixed by the solid soil.

*I* and Br loads in adjacent rivers give further support, a lower mean *I*/Br ratio in rivers (0.14; Piechulla, 2018) than in rain water indicates a higher Br than *I* export. In depths >20 cm, ratios in leachates rose to values of 1-1.5, suggesting that some Br was washed out to the river through topsoil and transitional soil horizons and did not reach the subsoil. All of this leads to the idea that Br is not only transported as organically bound Br, but also in inorganic form. Inorganic Br species were found to be more mobile and more common in soils than inorganic *I* species (Kabata-Pendias, 2011; Yuita et al., 1991).

Another explanation for rising *I*/Br ratios with depth might be the release of *I* as a result of lower OM content, OM decomposition and dehalogenation. The release of inorganic *I* by dehalogenation of OM was mainly observed in anoxic environments (Müller et al., 1996). Anoxic environments resulting from backwater are unlikely due to porous soils in the ReBAMB and steep slopes. Therefore, in the investigated soils the release of inorganic *I* is thought to only take place during the decomposition of OM.

Since profiles L1 and R5 were shallow and therefore missed a third sampling point in the depth profile, the increase of *I*/Br ratios in subsoils was not visible (Figure 14). Profile R4 constitutes

and exception, *I* seemed to be washed out more easily than Br in the topsoil horizon (5 cm) while the subsoil horizon (30 cm) showed the opposite situation. This might be attributed to higher DOC associated transport of *I* in the topsoil (5 cm) and higher mobility of inorganic Br species in the subsoil (30 cm).

However, it needs to be considered that concentrations of *I* and Br were extremely low, especially in subsoil horizons ( $\geq 30$  cm). Thus, small variations in concentration can cause a marked change in *I*/Br ratios. In summary, these findings show a stronger accumulation of *I* and a higher mobility of Br and therefore falsify hypothesis 4.

#### **4.3.2 *I* and Br species**

Since the *I*- and Br species could not be determined due to the low concentrations in leachates, only speculations can be provided on this. Presumably *I* and Br in the soil solution of the investigated soils occur mainly as SOI and organically bound Br. Among inorganic *I*- and Br species,  $\text{IO}_3^-$  and  $\text{Br}^-$  are likely dominant in soil solution. Whereas the latter is assumed to be more abundant due to the relative ease of *I* oxidation in relation to Br oxidation.  $\text{IO}_3^-$  was found to comprise 85 % of total soluble inorganic iodine under oxidising conditions (Yuita, 1992). SOI comprises more than half and up to 80 % of total soluble *I* in rain, *I* and  $\text{IO}_3^-$  fractions are smaller (Gilfedder et al., 2008). The major Br species in rain is  $\text{Br}^-$  (Gilfedder et al., 2011). As soon as *I* and Br are in contact with solid or DOM, inorganic forms are rapidly transformed into organic forms and stabilised in the uppermost centimeters of the soil (Hagedorn et al., 2015; Leri and Myneni, 2012; Shetaya et al., 2012). Dry deposition occurs through aerosols (Baker et al., 2001) in which SOI comprises the major *I* fraction (83-97 %; Gilfedder et al., 2008).

---

## 5 Outlook

For future investigations, sorption studies for *I* and Br in soil columns from tropical forests could reveal further knowledge on retention and mobilisation processes under different conditions. Variations in pH value and redox conditions would increase the understanding of *I*- and Br mobilisation dynamics. Furthermore, these experiments could enable investigations of waterflow paths and provide information on *I* and Br mobilisation and retention during matrix- and macropore-flow. Even higher concentrations of *I* and Br might be found in non-macropore regions in solid soil because mobilisation and transport might primarily take place in macropores.

The establishment of deeper soil profiles in ReBAMB could reveal *I* and Br concentration maxima in greater depths resulting from transport processes or relict topsoils buried by volcanic depositions. In this regard, volcanic ashes could be analysed, to assess their possible contribution to *I* and Br concentrations in soils. The analysis of their mineralogy could give information on their *I* and Br fixation potential due to volcanic glasses or allophanes.

The determination of *I* species in leachates would require HPLC columns with a detection limit of less than  $0.5 \mu\text{g L}^{-1}$  or an altered extraction method. *I* and Br species could give a more detailed insight from which binding partners *I* and Br are mobilised and in which form.

## 6 Conclusion

An overview of *I* soil chemistry in the soils of the ReBAMB can be seen in Figure 17. Almost all *I* and Br was fixed in the soil, with maximum water-leachable percentages of only 0.4 and 0.6 %, respectively. Mobility of *I* and Br was highest in topsoils (5-6 cm) and rapidly declined in subsequent soil horizons. *I* and Br seem to be rapidly fixed with OM in topsoils after incorporation with rainfall. Small amounts can be mobilised and transported to deeper soil horizons in association with DOC. Due to rapidly increasing contents of Fe-Oxides below topsoil horizons, *I*-DOC and Br-DOC associations are immobilised there. Fixation of organic *I*- and Br complexes by Fe-Oxides seems to play an important role in these soils. Br showed a higher mobility than *I*.

The results of this study demonstrate, that tropical soils, high in OM and Fe-Oxides, inhibit *I* and Br release and support *I* and Br accumulation. Reasons are the high *I* sorption and inputs due to high annual rainfall. The fixation of organic *I*- and Br complexes by Fe-Oxides seems to play the main role in *I* and Br retention in the soils of ReBAMB.

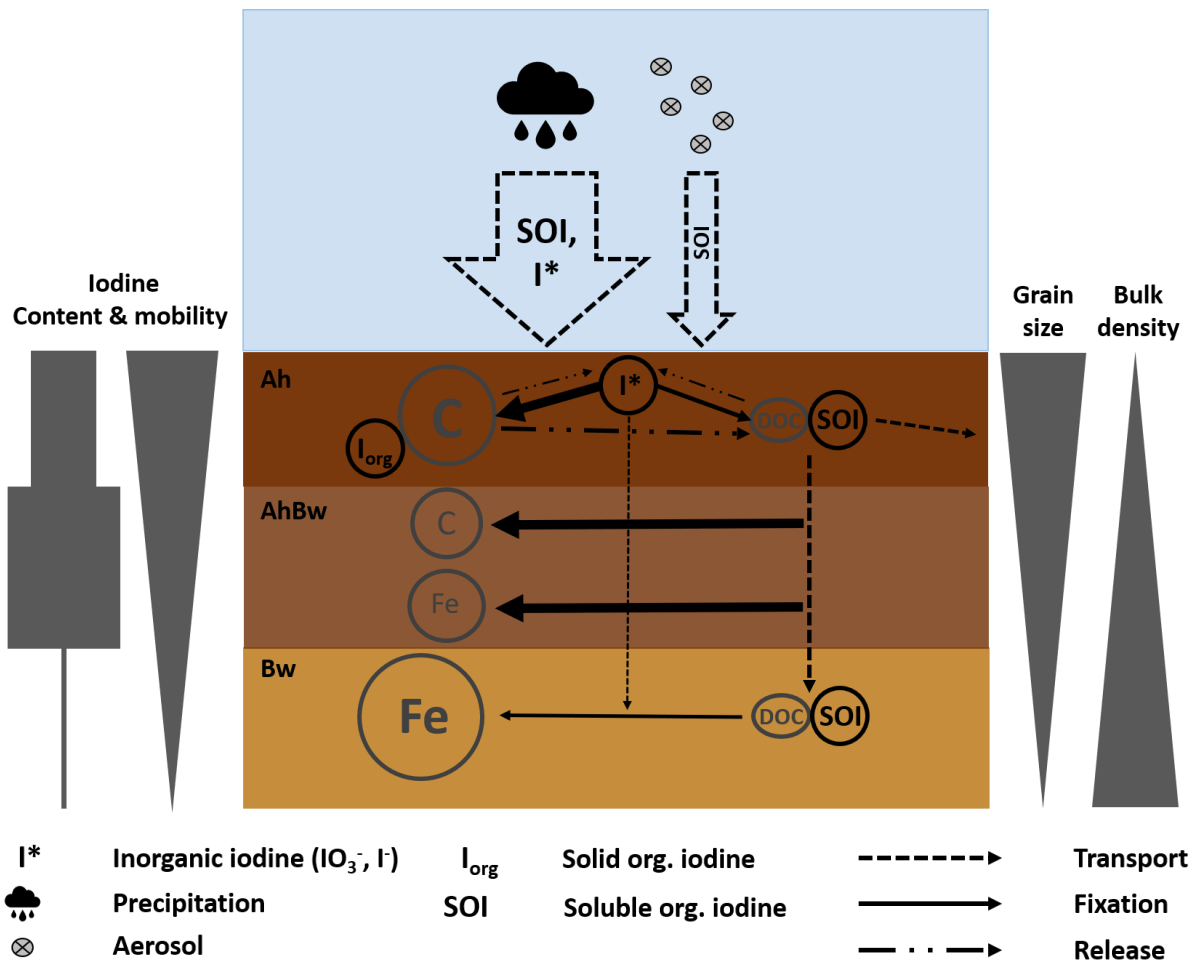


Figure 17: Overview of I chemistry in soils of the ReBAMB.

---

## References

- Ahn, Y.-B., Rhee, S.-K., Fennell, D.E., Kerkhof, L.J., Hentschel, U., Haggblom, M.M., 2003. Reductive Dehalogenation of Brominated Phenolic Compounds by Microorganisms Associated with the Marine Sponge *Aplysina aerophoba*. *Applied and Environmental Microbiology* 69 (7), 4159–4166.
- Aiuppa, A., Federico, C., Franco, A., Giudice, G., Gurrieri, S., Inguaggiato, S., Liuzzo, M., McGonigle, A.J.S., Valenza, M., 2005. Emission of bromine and iodine from Mount Etna volcano. *Geochem. Geophys. Geosyst.* 6 (8), n/a-n/a.
- Allard, S., Gallard, H., 2013. Abiotic formation of methyl iodide on synthetic birnessite: A mechanistic study. *The Science of the total environment* 463-464, 169–175.
- Andersson, M., Benoist, B. de, Darnton-Hill, I., Delange, F., 2007. Iodine deficiency in Europe: A continuing public health problem. World Health Organization, Geneva. Accessed 6 December 2017, 70 str.
- Aran, D., Gury, M., Jeanroy, E., 2001. Organo-metallic complexes in an Andosol: A comparative study with a Cambisol and Podzol. *Geoderma* 99 (1-2), 65–79.
- Baker, A.R., Tunnicliffe, C., Jickells, T.D., 2001. Iodine speciation and deposition fluxes from the marine atmosphere. *J. Geophys. Res.* 106 (D22), 28743–28749.
- Barry, P.J., Chamberlain, A.C., 1964. Deposition of Iodine onto plant leaves from air, in: Bustad, L.K. (Ed.), *Biology of Radioiodine*. Pergamon, pp. 69–77.
- Bauer, M., Blodau, C., 2006. Mobilization of arsenic by dissolved organic matter from iron oxides, soils and sediments. *Science of The Total Environment* 354 (2-3), 179–190.
- Benoist, B. de, 2004. Iodine status worldwide: WHO global database on iodine deficiency. Dept. of Nutrition for Health and Development, World Health Organization, Geneva. Accessed 6 December 2017, vii, 48.
- Biester, H., Keppler, F., Putschew, A., Martinez-Cortizas, A., Petri, M., 2004. Halogen Retention, Organohalogenes, and the Role of Organic Matter Decomposition on Halogen Enrichment in Two Chilean Peat Bogs. *Environ. Sci. Technol.* 38 (7), 1984–1991.
- Blum, W.E.H., 2012. *Bodenkunde in Stichworten*, 7., neu bearb. Aufl. ed. Hirt's Stichwortbücher. Borntraeger, Stuttgart, xi, 176.
- Broder, T., Biester, H., 2015. Hydrologic controls on DOC, As and Pb export from a polluted peatland – the importance of heavy rain events, antecedent moisture conditions and hydrological connectivity. *Biogeosciences* 12 (15), 4651–4664.
- Butler, A., Sandy, M., 2009. Mechanistic considerations of halogenating enzymes. *Nature* 460 (7257), 848–854.
- Camino-Serrano, M., Gielen, B., Luyssaert, S., Ciais, P., Vicca, S., Guenet, B., Vos, B.D., Cools, N., Ahrens, B., Altaf Arain, M., Borcken, W., Clarke, N., Clarkson, B., Cummins, T., Don, A., Pannatier, E.G., Laudon, H., Moore, T., Nieminen, T.M., Nilsson, M.B.,

- Peichl, M., Schwendenmann, L., Siemens, J., Janssens, I., 2014. Linking variability in soil solution dissolved organic carbon to climate, soil type, and vegetation type. *Global Biogeochem. Cycles* 28 (5), 497–509.
- Chai, J.Y., Muramatsu, Y., 2007. Determination of Bromine and Iodine in Twenty-three Geochemical Reference Materials by ICP-MS. *Geostand Geoanalyst Res* 31 (2), 143–150.
- Chang, H.-s., Xu, C., Schwehr, K.A., Zhang, S., Kaplan, D.I., Seaman, J.C., Yeager, C., Santschi, P.H., 2014. Model of radioiodine speciation and partitioning in organic-rich and organic-poor soils from the Savannah River Site. *Journal of Environmental Chemical Engineering* 2 (3), 1321–1330.
- Chebуркин, A.K., Shotyk, W., 1996. An Energy-dispersive Miniprobe Multielement Analyzer (EMMA) for direct analysis of Pb and other trace elements in peats. *Fresenius' Journal of Analytical Chemistry* 354 (5), 688–691.
- Cleveland, C.C., Townsend, A.R., Constance, B.C., 2004. Soil Microbial Dynamics in Costa Rica: Seasonal and Biogeochemical Constraints. *Biotropica* 36 (2), 184–195.
- Dahlgren, R.A., Saigusa, M., Ugolini, F.C., 2004. The Nature, Properties and Management of Volcanic Soils, in: Sparks, D.L. (Ed.), *Advances in agronomy*, vol. 82. *Advances in Agronomy v. 82*. Academic Press, San Diego, pp. 113–182.
- Dissanayake, C.B., Chandrajith, R., Tobschall, H.J., 2007. The iodine cycle in the tropical environment — implications on iodine deficiency disorders. *International Journal of Environmental Studies* 56 (3), 357–372.
- Eckelmann, H.:W., Sponagel, R.:H., Grottenthaler, W., Hartmann, K.-J., Hartwich, R., Janetzko, P., Joisten, H., Kühn, D., Sabel, K.-J., Traidl, R., Boden, H.:A.-h.-A. (Eds.), 2006. *Bodenkundliche Kartieranleitung. KA5*. Schweizerbart Science Publishers, Stuttgart, Germany.
- Emerson, H.P., Xu, C., Ho, Y.-F., Zhang, S., Schwehr, K.A., Lilley, M., Kaplan, D.I., Santschi, P.H., Powell, B.A., 2014. Geochemical controls of iodine uptake and transport in Savannah River Site subsurface sediments. *Applied Geochemistry* 45, 105–113.
- Food and Nutrition Board, Institute of Medicine, 2006. *Dietary Reference Intakes: The Essential Guide to Nutrient Requirements*. The National Academies Press, Washington, DC.
- Fuge, R., Johnson, C.C., 1986. The geochemistry of iodine - a review. *Environmental geochemistry and health* 8 (2), 31–54.
- Gérard, M., Caquineau, S., Pinheiro, J., Stoops, G., 2007. Weathering and allophane neof ormation in soils developed on volcanic ash in the Azores. *Eur J Soil Science* 58 (2), 496–515.
- Gilfedder, B.S., 2008. *Observations of Iodine Speciation and Cycling in the Hydrosphere*. Dissertation, Heidelberg.

- Gilfedder, B.S., Lai, S.C., Petri, M., Biester, H., Hoffmann, T., 2008. Iodine speciation in rain, snow and aerosols. *Atmos. Chem. Phys.* 8 (20), 6069–6084.
- Gilfedder, B.S., Petri, M., Wessels, M., Biester, H., 2010. An iodine mass-balance for Lake Constance, Germany: Insights into iodine speciation changes and fluxes. *Geochimica et Cosmochimica Acta* 74 (11), 3090–3111.
- Gilfedder, B.S., Petri, M., Wessels, M., Biester, H., 2011. Bromine species fluxes from Lake Constance's catchment, and a preliminary lake mass balance. *Geochimica et Cosmochimica Acta* 75 (12), 3385–3401.
- Hagedorn, F., Bruderhofer, N., Ferrari, A., Niklaus, P.A., 2015. Tracking litter-derived dissolved organic matter along a soil chronosequence using <sup>14</sup>C imaging: Biodegradation, physico-chemical retention or preferential flow? *Soil Biology and Biochemistry* 88, 333–343.
- Hu, Q., Moran, J.E., Blackwood, V., 2009. Geochemical Cycling of Iodine Species in Soils, in: , *Comprehensive Handbook of Iodine. Nutritional, Biochemical, Pathological and Therapeutic Aspects*. Academic Press, London, pp. 93–105.
- Hu, Q., Zhao, P., Moran, J.E., Seaman, J.C., 2005. Sorption and transport of iodine species in sediments from the Savannah River and Hanford Sites. *Journal of contaminant hydrology* 78 (3), 185–205.
- Humbert, G., Jaffrezic, A., Fovet, O., Gruau, G., Durand, P., 2015. Dry-season length and runoff control annual variability in stream DOC dynamics in a small, shallow groundwater-dominated agricultural watershed. *Water Resour. Res.* 51 (10), 7860–7877.
- Jansen, B., Nierop, K.G.J., Verstraten, J.M., 2005. Mechanisms controlling the mobility of dissolved organic matter, aluminium and iron in podzol B horizons. *Eur J Soil Science* 56 (4), 537–550.
- Johnson, C.C., 1980. The geochemistry of iodine and a preliminary investigation into its potential use as a pathfinder element in geochemical exploration. Ph.D. thesis, Aberystwyth.
- Kabata-Pendias, A., 2011. Trace elements in soils and plants. CRC Press, Boca Raton, xxviii, 520.
- Kabata-Pendias, A., Szeke, B., 2015. Trace elements in abiotic and biotic environments. CRC Press, Boca Raton, 440 S.
- Kaiser, K., Guggenberger, G., Zech, W., 1996. Sorption of DOM and DOM fractions to forest soils. *Geoderma* 74 (3-4), 281–303.
- Kaplan, D.I., Zhang, S., Roberts, K.A., Schwehr, K.A., Xu, C., Creeley, D., Ho, Y.-F., Li, H.-P., Yeager, C.M., Santschi, P.H., 2014. Radioiodine concentrated in a wetland. *Journal of environmental radioactivity* 131, 57–61.

- Keppeler, F., Eiden, R., Niedan, V., Pracht, J., Schöler, H.F., 2000. Halocarbons produced by natural oxidation processes during degradation of organic matter. *Nature* 403 (6767), 298–301.
- Kottek, M., Grieser, J., Beck, C., Rudolf, B., Rubel, F., 2006. World Map of the Köppen-Geiger climate classification updated. *metz* 15 (3), 259–263.
- Kricher, J., 2011. *Tropical ecology*. Princeton University Press, Princeton (NJ), viii, 632.
- Kuss, A., 2018. Verlagerung von Halogenspezies in verschiedenen Bodentypen. Masterarbeit, Braunschweig.
- Låg, J., Steinnes, E., 1976. Regional distribution of halogens in Norwegian forest soils. *Geoderma* 16 (4), 317–325.
- Leri, A.C., Myneni, S.C.B., 2012. Natural organobromine in terrestrial ecosystems. *Geochimica et Cosmochimica Acta* 77, 1–10.
- Leri, A.C., Ravel, B., 2015. Abiotic Bromination of Soil Organic Matter. *Environmental science & technology* 49 (22), 13350–13359.
- Leung, A.M., Braverman, L.E., 2014. Consequences of excess iodine. *Nature reviews. Endocrinology* 10 (3), 136–142.
- Li, H.-P., Brinkmeyer, R., Jones, W.L., Zhang, S., Xu, C., Ho, Y.-F., Schwehr, K.A., Kaplan, D.I., Santschi, P.H., Yeager, C., 2012a. Iodide Oxidizing Activity of Bacteria from Sub-surface Sediments of the Savannah River Site, SC, U.S.A. *Interdisciplinary Studies on Environmental Chemistry—Environmental Pollution and Ecotoxicology*, 89–97.
- Li, H.-P., Yeager, C.M., Brinkmeyer, R., Zhang, S., Ho, Y.-F., Xu, C., Jones, W.L., Schwehr, K.A., Otosaka, S., Roberts, K.A., Kaplan, D.I., Santschi, P.H., 2012b. Bacterial production of organic acids enhances H<sub>2</sub>O<sub>2</sub>-dependent iodide oxidation. *Environmental science & technology* 46 (9), 4837–4844.
- Martínez Cortizas, A., Vázquez, C.F., Kaal, J., Biester, H., Casais, M.C., Rodríguez, T.T., Lado, L.R., 2016. Bromine accumulation in acidic black colluvial soils. *Geochimica et Cosmochimica Acta* 174, 143–155.
- Miller, R.O., Kissel, D.E., 2010. Comparison of Soil pH Methods on Soils of North America. *Soil Science Society of America Journal* 74 (1), 310.
- Minasny, B., McBratney, A.B., Brough, D.M., Jacquier, D., 2011. Models relating soil pH measurements in water and calcium chloride that incorporate electrolyte concentration. *European Journal of Soil Science* 62 (5), 728–732.
- Moran, J.E., Oktay, S.D., Santschi, P.H., 2002. Sources of iodine and iodine 129 in rivers. *Water Resour. Res.* 38 (8), 24-1-24-10.
- Moulin, V., Reiller, P., Amekraz, B., Moulin, C., 2001. Direct characterization of iodine covalently bound to fulvic acids by electrospray mass spectrometry. *Rapid communications in mass spectrometry : RCM* 15 (24), 2488–2496.

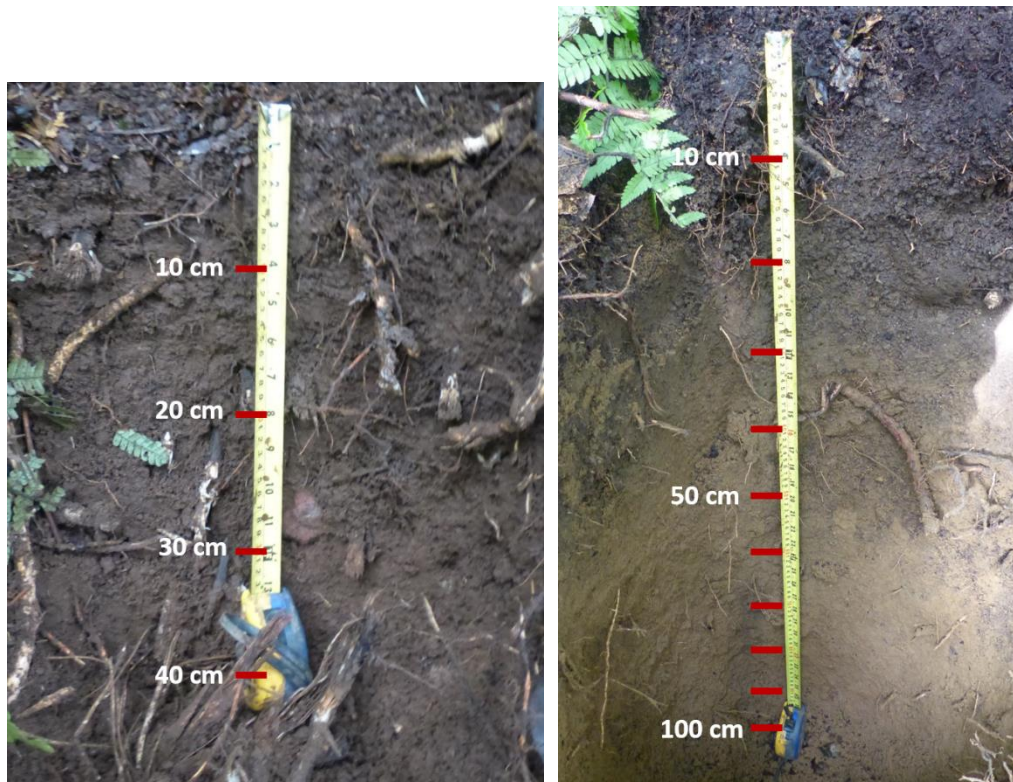
- Müller, G., Nkusi, G., Schöler, H.F., 1996. Natural Organohalogenes in Sediments. *J. Prakt. Chem.* 338 (1), 23–29.
- Muramatsu, Y., Yoshida, S., Fehn, U., Amachi, S., Ohmomo, Y., 2004. Studies with natural and anthropogenic iodine isotopes: Iodine distribution and cycling in the global environment. *Journal of environmental radioactivity* 74 (1-3), 221–232.
- Nanzyo, M., 2002. Unique properties of volcanic ash soils. *Global Environmental Research* 6, 99–112.
- Oades, J.M., 1988. The retention of organic matter in soils. *Biogeochemistry* 5 (1), 35–70.
- Paradellis, T., Panayotakis, N., 1980. Bromine absorption from air by plant leaves. *J. Radioanal. Chem.* 59 (1), 221–227.
- Piechulla, L., 2018. Sorption and mobilization of iodine in a tropical forest river catchment – A case study in Costa Rica. Master thesis, Braunschweig.
- Renneberg, A.J., Dudas, M.J., 2001. Transformations of elemental mercury to inorganic and organic forms in mercury and hydrocarbon co-contaminated soils. *Chemosphere* 45 (6), 1103–1109.
- Saiz-Lopez, A., Plane, J.M.C., Baker, A.R., Carpenter, L.J., Glasow, R. von, Martín, J.C.G., McFiggans, G., Saunders, R.W., 2012. Atmospheric chemistry of iodine. *Chemical reviews* 112 (3), 1773–1804.
- Santschi, P.H., Xu, C., Zhang, S., Schwehr, K.A., Grandbois, R., Kaplan, D.I., Yeager, C.M., 2017. Iodine and plutonium association with natural organic matter: A review of recent advances. *Applied Geochemistry* 85, 121–127.
- Sauvé, S., McBride, M., Hendershot, W., 1998. Soil Solution Speciation of Lead(II): Effects of Organic Matter and pH. *Soil Science Society of America Journal* 62 (3), 618.
- Scheffer, F., Schachtschabel, P., Blume, H.-P., Brümmer, G.W., Horn, R., Kandeler, E., Kögel-Knabner, I., Kretzschmar, R., Stahr, K., Thiele-Bruhn, S., Welp, G., Wilke, B.-M., 2010. *Lehrbuch der Bodenkunde*, 16. Auflage ed. Spektrum Akademischer Verlag, Heidelberg.
- Shetaya, W.H., Young, S.D., Watts, M.J., Ander, E.L., Bailey, E.H., 2012. Iodine dynamics in soils. *Geochimica et Cosmochimica Acta* 77, 457–473.
- Shoji, S., Nanzyo, M., Dahlgren, R.A., 1994. *Volcanic Ash Soils: Genesis, Properties and Utilization*, 1. Aufl. ed. Developments in soil science v.21. Elsevier textbooks, s.l., 0 pp.
- Shtangeeva, I., 2017. Bromine Accumulation in Some Crops and Grasses as Determined by Neutron Activation Analysis. *Communications in Soil Science and Plant Analysis* 48 (19), 2338–2346.
- Smyth, D., Johnson, C.C., 2011. Distribution of iodine in soils of Northern Ireland. *Geochemistry: Exploration, Environment, Analysis* 11 (1), 25–39.

- Stavber, S., Jereb, M., Zupan, M., 2008. Electrophilic Iodination of Organic Compounds Using Elemental Iodine or Iodides. *Synthesis* 2008 (10), 1487–1513.
- Steinberg, S.M., Kimble, G.M., Schmett, G.T., Emerson, D.W., Turner, M.F., Rudin, M., 2008. Abiotic reaction of iodate with sphagnum peat and other natural organic matter. *J Radioanal Nucl Chem* 277 (1), 185–191.
- Troyer, I. de, Amery, F., van Moorleghe, C., Smolders, E., Merckx, R., 2011. Tracing the source and fate of dissolved organic matter in soil after incorporation of a <sup>13</sup>C labelled residue: A batch incubation study. *Soil Biology and Biochemistry* 43 (3), 513–519.
- Tsai, C.C., Chen, Z.S., Kao, C.I., Ottner, F., Kao, S.J., Zehetner, F., 2010. Pedogenic development of volcanic ash soils along a climosequence in Northern Taiwan. *Geoderma* 156 (1-2), 48–59.
- van den Berg, L.J.L., Shotbolt, L., Ashmore, M.R., 2012. Dissolved organic carbon (DOC) concentrations in UK soils and the influence of soil, vegetation type and seasonality. *The Science of the total environment* 427-428, 269–276.
- Vitousek, P., 1986. Nutrient Cycling in Moist Tropical Forest. *Annual Review of Ecology and Systematics* 17 (1), 137–167.
- Vos, C., Don, A., Prietz, R., Heidkamp, A., Freibauer, A., 2016. Field-based soil-texture estimates could replace laboratory analysis. *Geoderma* 267 (Supplement C), 215–219.
- Wever, R., van der Horst, M.A., 2013. The role of vanadium haloperoxidases in the formation of volatile brominated compounds and their impact on the environment. *Dalton transactions (Cambridge, England : 2003)* 42 (33), 11778–11786.
- Whitehead, D.C., 1973. The sorption of iodide by soils as influenced by equilibrium conditions and soil properties. *J. Sci. Food Agric.* 24 (5), 547–556.
- Whitehead, D.C., 1978. Iodine in soil profiles in relation to iron and aluminium oxides and organic matter. *Journal of Soil Science* 29 (1), 88–94.
- Whitehead, D.C., 1981. The volatilisation, from soils and mixtures of soil components, of iodine added as potassium iodide. *Journal of Soil Science* 32 (1), 97–102.
- Whitehead, D.C., 1984. The distribution and transformations of iodine in the environment. *Environment International* 10 (4), 321–339.
- Wisniak, J., 2002. The history of Br from discovery to commodity. *Indian Journal of Chemical Technology* 9, 263–271.
- Xu, C., Miller, E.J., Zhang, S., Li, H.-P., Ho, Y.-F., Schwehr, K.A., Kaplan, D.I., Otosaka, S., Roberts, K.A., Brinkmeyer, R., Yeager, C.M., Santschi, P.H., 2011a. Sequestration and remobilization of radioiodine (<sup>129</sup>I) by soil organic matter and possible consequences of the remedial action at Savannah River Site. *Environmental science & technology* 45 (23), 9975–9983.

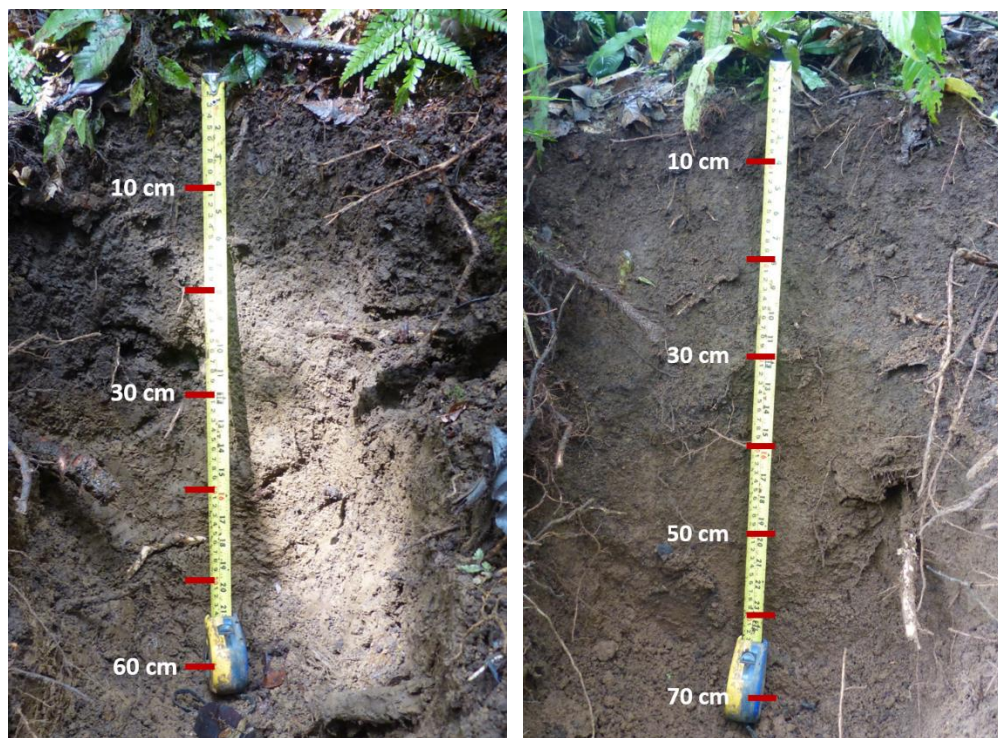
- 
- Xu, C., Zhang, S., Ho, Y.-F., Miller, E.J., Roberts, K.A., Li, H.-P., Schwehr, K.A., Otsuka, S., Kaplan, D.I., Brinkmeyer, R., Yeager, C.M., Santschi, P.H., 2011b. Is soil natural organic matter a sink or source for mobile radioiodine (<sup>129</sup>I) at the Savannah River Site? *Geochimica et Cosmochimica Acta* 75 (19), 5716–5735.
- Yamada, H., Kiriya, T., Onagawa, Y., Hisamori, I., Miyazaki, C., Yonebayashi, K., 1999. Speciation of iodine in soils. *Soil Science and Plant Nutrition* 45 (3), 563–568.
- Yoshida, S., Muramatsu, Y., Uchida, S., 1992. Studies on the sorption of iodide and iodate onto Andosols. *Water Air Soil Pollut* 63 (3-4), 321–329.
- Yuita, K., 1983. Iodine, bromine and chlorine contents in soils and plants of Japan. *Soil Science and Plant Nutrition* 29 (4), 403–428.
- Yuita, K., 1992. Dynamics of iodine, bromine, and chlorine in soil. *Soil Science and Plant Nutrition* 38 (2), 281–287.
- Yuita, K., Kihou, N., 2005. Behavior of Iodine in a Forest Plot, an Upland Field, and a Paddy Field in the Upland Area of Tsukuba, Japan: Vertical Distribution of Iodine in Soil Horizons and Layers to a Depth of 50 m. *Soil Science and Plant Nutrition* 51 (4), 455–467.
- Yuita, K., Tanaka, T., Abe, C., Aso, S., 1991. Dynamics of iodine, bromine, and chlorine in soil. *Soil Science and Plant Nutrition* 37 (1), 61–73.
- Zech, W., Schad, P., Hintermaier-Erhard, G., 2014. *Böden der Welt*.

## Appendix

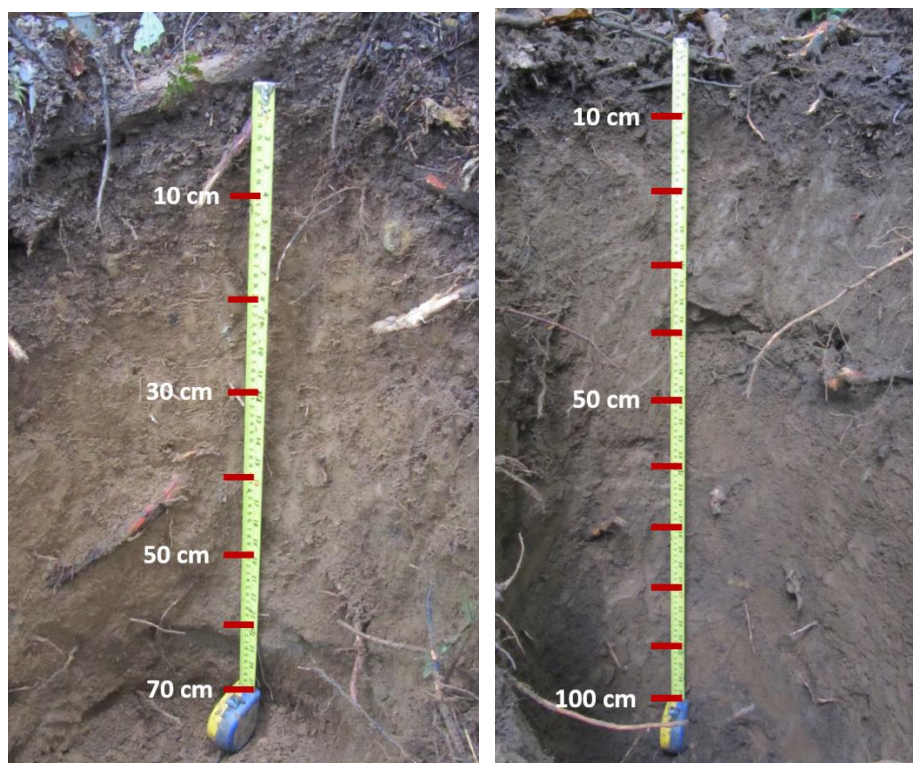
### **Soil profiles**



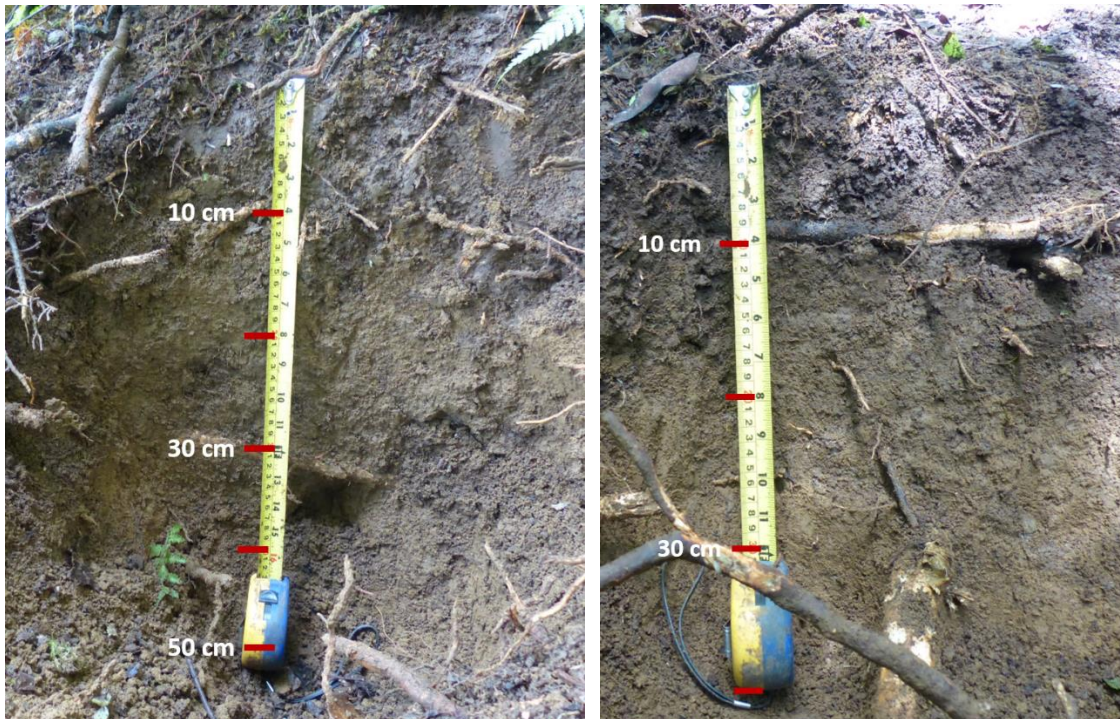
*Appendix 1: Soil profiles L1 (left, Colluvic Cambisol) and L2 (right, Haplic Cambisol), ReBAMB, Costa Rica, June 2017.*



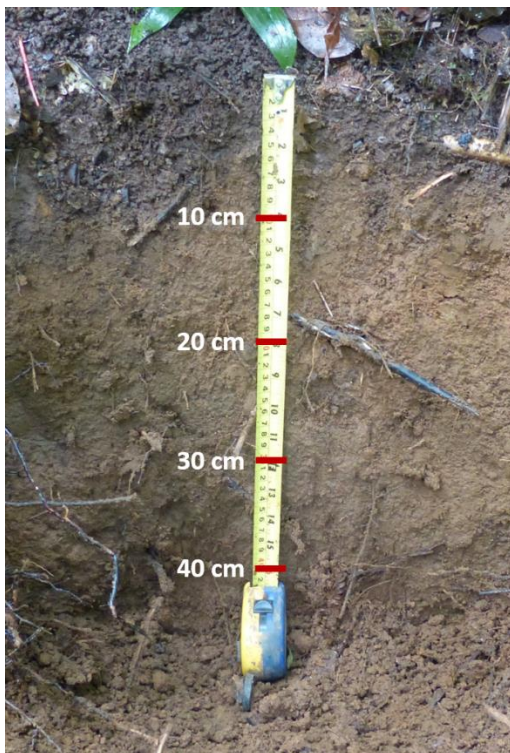
Appendix 2: Soil profiles L3 (left, Colluvic Cambisol) and L4 (right, Colluvic Cambisol), ReBAMB, Costa Rica, June 2017.



Appendix 3: Soil profiles R1 (left, Cambisol) and R2 (right, Haplic Cambisol), ReBAMB, Costa Rica, June 2017.



*Appendix 4: Soil profiles R3 (left, Cambisol) and R4 (right, Dystric Cambisol), ReBAMB, Costa Rica, June 2017.*



*Appendix 5: Soil profile R5 (Cambisol), ReBAMB, Costa Rica, June 2017.*

**Nutrient concentrations**

Appendix 6: Iron (Fe), Chloride (Cl<sup>-</sup>), Nitrate (NO<sub>3</sub><sup>-</sup>) and Sulfate (SO<sub>4</sub><sup>2-</sup>) concentrations in leachates.

Soil profile	Fe [μg L <sup>-1</sup> ]	Cl <sup>-</sup> [mg L <sup>-1</sup> ]	NO <sub>3</sub> <sup>-</sup> [mg L <sup>-1</sup> ]	SO <sub>4</sub> <sup>2-</sup> [mg L <sup>-1</sup> ]
L1 Ah	7.11	0.89	16.29	1.15
L1 II AhBw	0.16	0.56	3.22	0.49
L2 Ah	44.67	1.37	7.11	3.32
L2 AhBw	1.29	1.01	7.40	0.70
L2 Bw1	1.24	0.84	0.49	1.11
L2 Bw2	0.28	0.71	0.21	1.08
L3 Ah	1.50	0.72	19.37	1.77
L3 II AhBw	2.01	0.52	5.57	1.76
L3 Bw	2.19	1.06	1.00	1.74
L4 Ah	1.17	0.73	17.95	2.32
L4 II AhBw	8.37	0.72	3.87	1.64
L4 Bw	8.34	1.12	1.33	0.85
R1 Ah	2.01	0.93	21.39	1.69
R1 Bw	5.06	0.70	2.33	0.48
R2 Ah	1.47	0.70	15.02	2.05
R2 AhBw	0.61	0.64	4.59	1.67
R2 Bw	42.31	0.95	0.66	0.80
R3 Ah	0.66	0.92	10.96	1.20
R3 Bw1	0.33	0.90	1.92	0.51
R3 Bw2	0.68	0.64	0.60	1.01
R4 Ah	21.64	1.47	23.73	2.15
R4 Bw	0.13	1.59	1.71	1.77
R5 Ah	1.15	0.68	16.04	2.32
R5 Bw	2.08	0.68	2.00	1.28

\* Blum (2012)

Appendix 7: Main- and trace nutrient concentrations in solid soil samples.

<i>Soil profile</i>	<i>Fe</i> [g kg <sup>-1</sup> ]	<i>N</i> [g kg <sup>-1</sup> ]	<i>K</i> [g kg <sup>-1</sup> ]	<i>Ca</i> [g kg <sup>-1</sup> ]	<i>Mn</i> [mg kg <sup>-1</sup> ]	<i>Cu</i> [mg kg <sup>-1</sup> ]	<i>Zn</i> [mg kg <sup>-1</sup> ]
L1 Ah	118	10.8	2	10	1267	137	101
L1 II AhBw	87	3.7	2	8	939	108	72
L2 Ah	43	20.3	1	7	394	41	56
L2 AhBw	80	9.9	1	7	522	73	58
L2 Bw1	109	4.4	2	7	594	76	60
L2 Bw2	126	2.4	1	5	325	79	56
L3 Ah	95	13.7	2	8	1370	90	71
L3 II AhBw	137	9.6	2	7	1293	129	80
L3 Bw	176	4.0	1	6	1661	193	80
L4 Ah	70	15.4	2	11	1347	81	73
L4 II AhBw	72	7.0	2	15	1276	73	81
L4 Bw	151	5.6	1	7	1461	205	77
R1 Ah	100	11.1	1	8	762	93	76
R1 Bw	127	5.0	1	7	776	111	77
R2 Ah	108	9.5	2	8	1584	105	81
R2 AhBw	94	7.3	2	9	1430	93	80
R2 Bw	152	4.5	1	5	1584	132	72
R3 Ah	105	9.5	2	7	752	109	75
R3 Bw1	125	5.7	2	10	1172	114	94
R3 Bw2	139	4.3	2	6	1025	131	82
R4 Ah	120	11.2	1	7	723	131	98
R4 Bw	134	4.3	1	6	864	142	106
R5 Ah	120	9.9	2	10	1960	113	130
R5 Bw	110	5.8	2	8	1591	110	96

\* Blum (2012)